Maaß and Kraume (2011), Determination of breakage rates using single drop experiments, Chem. Eng. Sci. DOI: 10.1016/j.ces.2011.08.027

DETERMINATION OF BREAKAGE RATES USING SINGLE DROP EXPERIMENTS

Sebastian Maaß[1*] and Matthias Kraume[1]

[1]Technische Universität Berlin, Straße des 17. Juni 135, Sekr. MA 5-7, Chair of Chemical and Process Engineering, Sekr. MA 5-7, 10623 Berlin, Germany

[*]corresponding author (sebastian.maass@tu-berlin.de)

ABSTRACT

An evaluation of several breakage rates from the literature based on single drop experiments was carried out. This data was collected in a single drop breakage cell under turbulent conditions, comparable to those in a stirred tank. For a constant initial diameter and flow velocity at least 750 single drops have been investigated to measure the breakage time and probability, using high-speed imaging. These results were used for the determination of breakage rates by the product of the inverse of breakage time and the breakage probability. The same subdivision was carried out for the literature models. These differentiations in the analysis showed that published models for the breakage probability are more or less similar and in good agreements with the experimental results. Proposed approaches for the breakage time are contrary. The experiments support the assumption of some researchers that the breakage time rise with increasing drop diameter. The magnitude of the predicted values of the breakage time for all kind of models is one or more magnitudes higher than experimental results in this study and from literature. Furthermore the influence of the physical properties, like viscosity or interfacial tension, is only poorly reflected in the available models. These analysis results lead to an improved breakage time model, which takes into account different breakage mechanisms and the influence of viscosity and interfacial tension. Combined with a breakage probability from literature, this new model leads to an excellent prediction of the breakage rate for the investigated single drops. Inconvenience

KEYWORDS

drop breakage, population balance modeling, breakage kernel model, breakage time, parameter estimation, Rushton turbine

1 INTRODUCTION

The dispersion of an immiscible fluid in a turbulent liquid flow is commonly found in many technical as well as natural processes, with major importance for the chemical, pharmaceutical, mining, petroleum, and food industries. The behavior of such liquid-liquid systems and, more specifically, of their dispersed phases, is the result of a complex combination of processes that occur at the level of a single drop (Ribeiro et al. 2011). Complete models for these events as a function of power input, material, and process parameters are rare and relatively inaccurate.

An extremely useful modeling approach is the population balance equation (PBE). It has been widely used to predict drop size distributions in several applications (Ramkrishna 2000). The key challenge associated with the formulation of predictive PBE models is the experimental determination of unknown drop breakage and coalescence functions as submodels in the PBE. While drop breakage under laminar conditions has been extensively studied, predictive models for drop breakage and coalescence under turbulent conditions are lacking or are rather inaccurate (Raikar et al. 2009). Many contradictory ideas for breakage and coalescence rates have been published over the last decades. A broad and detailed overview of existing functions is given in two papers by Liao and Lucas (drop breakage modeling - Liao and Lucas 2009, drop coalescence modeling - Liao and Lucas 2010). In this work we want to focus on analyzing the drop breakage rates, used as submodels in the PBE.

More recent approaches give a monotonic relation between the breakage rate and the drop size while the older ones exhibit a maximum as the parent diameter increases, which is already considered erroneous in the literature (Chen et al. 1998; Tsouris and Tavlarides 1994). However, the argument is open to question. Additionally, the quantitative difference between PBE models can be several orders of magnitude and need to be fixed by parameter adaptation. This problem was recently discussed by Ribeiro et al. (2011) who proposed the need for separate determination of these parameters.

Breakage rates will be analyzed in this study separately from coalescence in a single drop breakage cell (Maaß et al. 2007). This allows the precise determination of the magnitude and structure of those models. Therefore, the study is organized as follows.

A short overview of existing approaches of the breakage rate is given in section two after a short introduction into population balances. For a deeper understanding of the physical meaning, these models are subdivided as proposed in literature (Coulaloglou and Tavlarides 1977) into the inverse of the breakage time and the breakage probability. Experimental results from the literature for breakage time and probability are given in the second part of section two. After the presentation of the single drop measurement cell in section three, the measurement and parameter estimation procedures are described. Section four presents experimental single drop results for the breakage probability and time. These results are compared with literature models. In the fifth section a new breakage time model is derived, based on the insights from the experimental results. The sixth section combines all results in the presentation of the breakage rates.

2 DROP BREAKAGE IN TURBULENT SYSTEMS

Numerous experiments and simulations of single fluid particle deformation and breakage have been carried out in parallel bands or cylinder devices (see the pioneer work from Taylor (1934)). The advantages of detailed drop breakup experiments under steady and transient shear or elongation, as well as mixed flow conditions at low Reynolds numbers, are obvious. The extremely well defined conditions allow a clear connection between the flow field and

the particle deformation and therewith a connection with the responsible breakage mechanism. However, the aim of this investigation is the validation of breakage rate models used for simulations of drop sizes in stirred vessels with anisotropic turbulence. Therefore, breakage rate models for turbulent breakup will be discussed in this chapter after a short introduction into population balances.

2.1 Breakage dominant formulation of the population balance

Population balance equations describe the temporal variation in dispersed phase characteristics where the dispersed phase is considered as an assembly of particles whose individual identities are being continually changed over time. The population balance equations belong to a subcategory of equations known as partial differential equations.

The PBE in a batch reactor can be expressed as a univariate PBE, which only considers size change of the individuals:

$$\frac{\partial f(V_p)}{\partial t} = B_b(V_P,t) - D_b(V_P,t) + B_c(V_P,t) - D_c(V_P,t) \tag{1}$$

Here B_b, D_b, B_c and D_c are the birth rate by breakage, death rate by breakage, birth rate by coalescence, and death rate by coalescence, respectively. Each of these terms is a single kernel which contains further sub models. As this work focuses on drop breakage, the birth and death term by this process are described as follows:

$$\frac{\partial f(V_p)}{\partial t} = \int_{V_P'}^{V_{P,max}'} \nu(V_p')\,\beta(V_p, V_p')\,g(V_p')\,f(V_p',t)\,dV_P - g(V_p)\,f(V_p,t) \tag{2}$$

where $g(V_P)$ is the breakage rate, $\nu(V_P)$ is the number of dispersed fluid entities formed upon breakage of a particle V_P, and $\beta(V_P,V_P')$ is the size distribution of daughter fragments formed from the breakage of a particle V_P. A more detailed discussion of the population balance in general can be found in Ramkrishna (2000).

2.2 Modeling of drop breakage

The mechanistic model for the drop breakage rate $g(d_P)$ proposed by Coulaloglou and Tavlarides (1977) is based on the assumption that $g(d_P)$ is a product of the fraction of the total number of breaking drops, and the reciprocal time needed for the drop breakage to occur:

$$g(d_P) = \left(\frac{1}{\text{breakage time}}\right) \cdot \left(\frac{\text{fraction of}}{\text{breaking drops}}\right) = \frac{1}{t_b} \cdot \frac{N_b}{N_{tot}} \tag{3}$$

The fraction of breaking drops can be measured directly in the breakage channel and is assumed to be proportional to the fraction of turbulent eddies colliding with the drops that have a turbulent kinetic energy greater than the drop surface energy. The drop breakage time t_b is the time that is needed to breakup an initially undeformed drop (Stork 2005). It is derived from Batchelor's equation for the motion of two lumps in the turbulent field (Batchelor 1952). The distance for two different breakage events (equally and unequally sized breakage) is shown exemplarily in Figure 1.

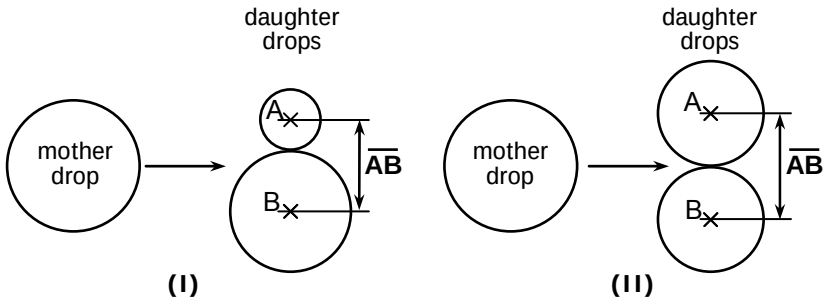

Figure 1 – Initial distance between the centre points A and B for binary drop breakage: exemplarily unequally sized breakage (I) and equally sized breakage (II). The mass balance is fulfilled for both events.

The increasing distance between the two lumps or particles is proportional to the time, the energy dissipation rate ε, and the initial distance of the measurement, which is equal to t_b for a drop breakage event.

$$\left(\overline{AB'}(t)\right)^2 \propto \left(\overline{AB}\cdot\varepsilon\right)^{2/3}\cdot t^2, \text{ with } \overline{AB}(t=t_b) \tag{4}$$

For equally sized daughter drops after a binary breakage, the distance between both daughter particles is equal to their diameter d'_P, which is equal to d''_P. This assumption is a valid simplification, since possible distance variation is low (see Figure 1). The appearance of unequally sized breakage events at all is not neglected by this assumption, since it is determined by the daughter drop size distribution β explained in equation (2).

With this assumption and the introduction of a proportionality constant c, the breakage time can be calculated with the following equation:

$$t_b = c\cdot\frac{d_P^{2/3}}{\varepsilon^{1/3}} \tag{5}$$

Note that the dispersed phase fraction $\varphi \rightarrow 0$ due to the analysis of single drops. Therefore, it is not displayed in the breakage rate equations in this study. The overall breakage rate by Coulaloglou and Tavlarides (1977) is written as follows:

$$g(d_p) = c_{1,b}\,\frac{\varepsilon^{1/3}}{d_P^{2/3}}\exp\left(-\frac{c_{2,b}\gamma}{\rho_d\,\varepsilon^{2/3}d_P^{5/3}}\right) \tag{6}$$

Although they reported a dependence of the breakage probability (exponential term in equation (6)) on the dispersed phase density ρ_d, Lasheras et al. (2002) criticize this in general and postulate that the dependency should be on the continuous phase density ρ_c. Vankova et al. (2007) took this thesis into account and extended equation (5) by the densities, based on derivations from Levich (1962) for the breakup of a liquid mass of arbitrary shape by random waves on the liquid surface (Levich 1962). Opposed to the critics by Lasheras et al. (2002), this was implemented in the pre-exponential term for dispersed phases with low viscosities:

$$t_b = \frac{1}{c_{1,b}}\cdot\frac{d_P^{2/3}}{\varepsilon^{1/3}}\sqrt{\frac{\rho_d}{\rho_c}} \tag{7}$$

This formulation is still very similar to the original equation proposed by Coulaloglou and Tavlarides (1977). Also Raikar et al. (2009) extended the model in equation (5). They introduced the dispersed phase density in the pre-exponential term, describing the breakage time as follows:

$$t_b = \frac{1}{c_{1,b}} \cdot \frac{d_P^{2/3}}{\varepsilon^{1/3}} \cdot \rho_d^{1/3} \tag{8}$$

The dimension of the numerical constant c is adapted into $kg^{1/3} \cdot m^{-1}$. In contradiction to these works is the assumption of Chen et al. (1998), who set the breakage time as constant but introduced the dispersed phase viscosity into the formulation of the breakage probability P, to take drop damping into account:

$$P = \frac{N_b}{N_{tot}} = \exp\left(- \frac{c_{2,b}\gamma}{\rho_d {d_P}^{5/3} \varepsilon^{2/3}} - \frac{c_{3,b}\eta_d}{\rho_d {d_P}^{4/3} \varepsilon^{1/3}} \right) \tag{9}$$

Equation (9) is a monotonously growing function and contains the influence of viscosity in contrast to the model of Coulaloglou and Tavlarides (1977). However, the presented equations (5)- (9) are mechanistic models.

Another class of models considers the random breaking of the initial mother drop in various disjointed elements in one or several steps. A key assumption, introduced by Narsimhan et al. (1979), is that the breaking drops follow a Poisson process (Ross 1983). This is a stochastic process with a Poisson distribution. This assumption was generally criticized by Villermaux (2007). He stated that nature does not split liquid volumes at random. With experimental high-speed images of breaking drops he showed that minute but significant differences exist between experimental data and assumed stochastic distributions, like Poisson or log-normal distributions (Villermaux 2007). However, the breakage rate of Narsimhan et al. (1979) was used by several authors (see for example Ruiz and Padilla 2004) with good drop size prediction results:

$$g(d_p) = c_{1,b} \cdot \mathrm{erfc}\left(\frac{c_{2,b}}{d_P^{5/6} \varepsilon^{1/3}} \sqrt{\frac{\gamma}{\rho_c}} \right) \tag{10}$$

Its stochastic nature was already overworked in two steps by Alopaeus et al. (2002). First, they combined the original kernel with the consideration of viscous forces according to Calabrese et al. (1986), while the original development was based on the assumption that viscous forces are negligible. Secondly, they enhanced the pre erfc-term. The equation was modified to include the energy dissipation dependence for the eddy-drop collision. They found a dependency of $\varepsilon^{1/3}$ in the pre erfc-parameter, which is also predicted by the turbulence theory. No significant diameter dependency for $c_{1,b}$ in equation (11) was found (Alopaeus et al. 2002). Note that by this extension the original unit of the numerical constant $c_{1,b}$ changes from $[s^{-1}]$ to $[m^{-2/3}]$.

$$g(d_p) = c_{1,b}\varepsilon^{1/3} \cdot \operatorname{erfc}\left(\sqrt{\frac{c_{2,b}\gamma}{\rho_c d_P^{5/3}\varepsilon^{2/3}} + \frac{c_{3,b}\eta_d}{\sqrt{\rho_c\rho_d}\, d_P^{4/3}\varepsilon^{1/3}}}\right) \tag{11}$$

The used function is the complementary of the error function, also named probability integral (see Abramowitz et al. (1984) p. 84ff for more details), which is defined as follow:

$$\operatorname{erfc}(d_p) = 1 - \operatorname{erf}(d_p) = \frac{2}{\sqrt{\pi}} \int_0^{\infty} e^{-t^2} dt \tag{12}$$

The presented breakage rate in equation (11) is a transitional probability (Narsimhan et al. 1979). The probability of breaking drops per time interval t is given by the erfc-term. A closer examination of this part and a comparison with the drop breakage probability by Chen et al. (1998) in equation (9) reveals an interesting similarity. The physical description of the drop breakage event controlled by the surface and viscous forces described by both author groups are absolutely equal.

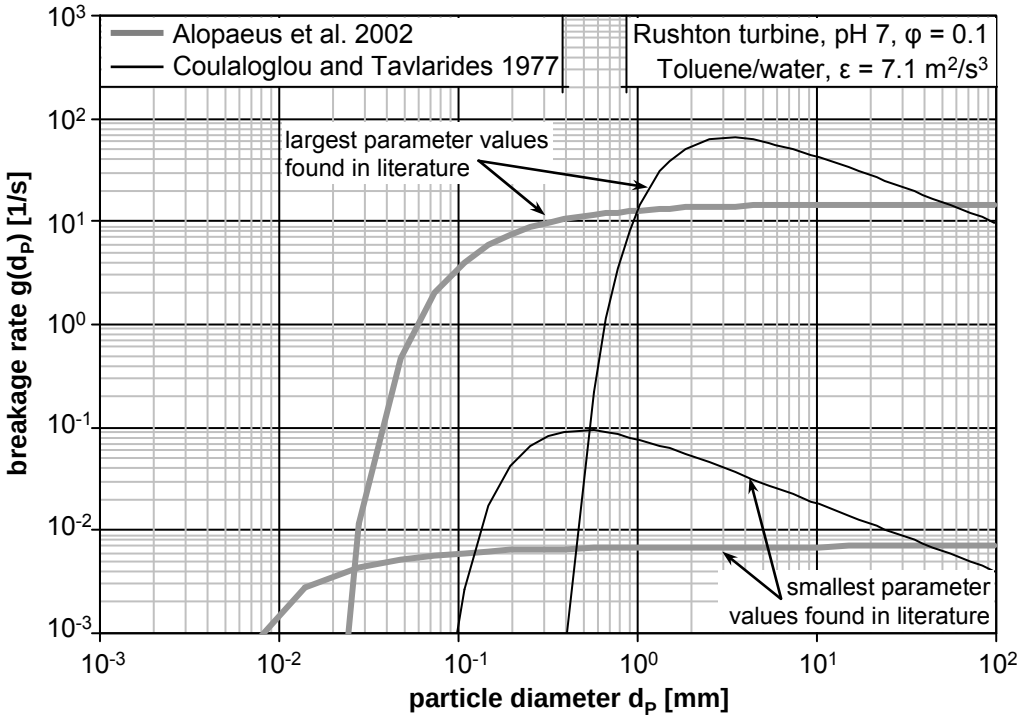

Figure 2 – Breakage rates from literature for constant physical properties with opposing mathematical behavior.

Figure 2 summarizes the variety of the discussed models and their differences in magnitude. Two different models are displayed. The physical properties have been set constant with a toluene/water system and a constant energy dissipation rate. The curve shapes of the different breakage rates over the particle diameter contradict each other. The breakage rate by Coulaloglou and Tavlarides (1977) predicts a maximum for a certain drop size. The model of Alopaeus et al. (2002) does not. The size for the maximum stable diameter varies strongly

(8 – 400 μm). The differences in the magnitude of the predicted values for the same breakage rate model are caused by the different values of the parameters used. The constants used in Figure 2 reflect the maximum and minimum value found in literature for predicting particle sizes in multiphase systems. A short overview of the parameters (minimum and maximum values) used in literature is given in Table 8 in Appendix A. These confusing and contradicting results should be clarified. The aim of this investigation is therefore to determine the curve shape over the particle diameter and the magnitudes of breakage rates using single drop experiments.

2.3 Experimental investigations

Different experimental investigations have been carried out to analyze the breakage rates in the PBE. In this chapter we want to focus especially on single drop breakage results which have already been carried out. These studies give a first insight into the breakage mechanisms without affecting the coalescence effects and allow a comparison with the single drop experiments in this study.

Bahmanyar and Slater (1991) observed breakage of single drops in a rotating disc contactor. Due to the low time resolution of their measurement techniques (capillary and video technique) they were not able to determine breakage times connected to a single breakage event. The breakage probabilities of the experimentally investigated drop swarms are a function of the stirrer disc Weber number $We_{str} = \rho_c n^2 D^3/\gamma$ and they increase with increasing We monotonically.

Schmidt et al. (2006) used their breakage probabilities determined experimentally in a rotating disc column to develop a correlation for the breakage rate, taking viscosity effects into account. Their results show that the interfacial tension especially has a much more significant influence than the viscosity of the dispersed phase.

The influence of mass transfer on single drop breakage was investigated by Gourdon and Casamatta (1991). Their experimental work was carried out in a pulsed sieve-plate pilot column with a water-acetone-toluene system. All achieved breakup results were gathered in a single correlation of the breakage probability. They displayed that by varying mass transfer intensity, direction, and sieve-plate characteristics, the breakage probability is an exponential function of the drop Weber number $We_{dr} = \rho_c w^2 d_p^3/\gamma$ (see equation (13)). The drop velocity $w = d_P^{1/3}\varepsilon^{1/3}$ can be replaced after the turbulence theory.

$$P = \exp\left(-\frac{C_1}{We_{dr}}\right) = \exp\left(-\frac{C_1\gamma}{\rho_c \varepsilon^{2/3} d_P^{5/3}}\right) \tag{13}$$

These results support the breakage probabilities used by authors like Coulaloglou and Tavlarides (1977), who assumed the same dependencies of P on d_P and ε (compare equation (13) with equation (6)).

Galinat et al. (2005) investigated the breakage probability, the number of daughter drops and the resulting daughter drop size distribution as a function of the flow velocity and mother drop diameter. The increase of diameter and velocity led to a strong increase of the breakage probability. The expression for the breakage probability based on the experimental results follows the structure and weighting of the breakage probability in equation (6).

Andersson and Andersson (2006) investigated the dynamics of bubble and drop breakage with a high-speed technique. The breakage time, deformation and daughter drop size distribution were measured with frame rates between 500 and 4000 frames per second (fps) under homogeneous turbulence and energy dissipation rates in a reactor, developed in their laboratory. This continuous reactor consisted of repeating identical small mixing elements. It was specifically designed to study the effect of turbulence on drop breakage, since turbulence is continuously produced and dissipated along the reactor (Andersson et al. 2004). The highest values for the breakage time were found for the lowest flow (100 L/h) and the highest dispersed phase viscosity (6.5 mPa·s) of 10.9 ms. The interpretation of the work by Anderson and Anderson (2006) is difficult, because no definition for their breakage time nor the overall amount of investigated events is given by the authors. However, the work is clearly presented and gives an excellent overview of the experimental analysis on drop breakage.

The studies by Eastwood et al. (2004) deal with drop breakage in a turbulent liquid jet. They found that drops were considerably elongated before breakage. The deformation or stretching rose with increasing drop viscosity. The stretching occurred on scales comparable to the turbulent integral length scale, and some deformed drops seemed to rotate with the flow structures. They propose that the elongated particle break is caused by capillary effects resulting from differences in the radius of curvature along their length. Therefore, they scale the breakage time with the capillary time and draw similarities to laminar breakage.

Konno et al. (1983) used high-speed photography to directly observe drop breakage events in stirred vessels. To avoid coalescence they always used a dilute liquid/liquid system with a dispersed phase fraction lower than 0.2 %. The images were taken with up to 4000 fps. The breakage time, drop path and the number of drops per breakage event were recorded. The investigated mother drop sizes were in the range of 0.26 - 1.0 mm. Konno et al. (1983) observed breakage times always lower than 7 ms. The major drawback of their approach is the insufficient number of breakage events for statistically meaningful results.

A summary of experimentally determined breakage times from literature is given in Table 1. Generally, the obtained results of t_b for the various systems are almost all in the same range (between 3.4 and 100 ms). The differences in the absolute values for the same physical systems investigated by different researchers are mainly caused by the different fluid dynamics and set-ups used, also given in Table 1.

Table 1 – Results for breakage times from liquid-liquid experiments

Literature reference	experimental set-up	system	η_d/η_c [-]	γ [mN/m]	frame rate [fps]	Reynolds number Re [10^3]	t_b [ms]
Andersson and Andersson 2006	static mixer	water dodecane	1.5	53	1000	52	7.6
Andersson and Andersson 2006	static mixer	water octanol	6.5	8.5	500	52	5.6
Eastwood et al. 2004	pipe flow	water heptane	0.5	48	1000	39	4
Eastwood et al. 2004	pipe flow	water silicone oil	9.7	35	1000	39	4
Eastwood et al. 2004	pipe flow	water silicone oil	50.9	37	1000	39	6
Galinat et al. 2005	pipe flow	water n-heptane	0.5	23.6	456	6.4	48
Hesketh et al. 1991	pipe flow	water silicone oil	19	30.3	1200	84	10-100
Konno et al. 1983	stirred tank	water o-xylene	0.8	34	4000	270	3.4

3 MATERIALS AND METHODS

3.1 Experimental set-up

For more detailed understanding and precise parameter determination, breakage rates have been analyzed separately from coalescence in a single drop breakage cell. A single blade representative of a section of a Rushton turbine is fixed in a rectangular channel (see Figure 3). This set-up reflects the flow field in the impeller region, where turbulent pressure fluctuation, shear flow in a thin layer on the impeller blade, and the two-dimensional (2D) elongational flow field in front of the rotating blade are the major drop breakage reasons. All these phenomena were assumed to occur simultaneously (Kumar et al. 1998). When these three mechanisms interfere with each other need to be analyzed, to evaluate the breakage phenomena precisely for stirred tank applications. This can be done in the breakage cell.

The relative velocity between blade and liquid flow was approximately 1.0 to 3.0 m/s, a range typical for the flow field around the stirrer blade in a stirred tank. Also, the local energy dissipation rates of both the channel and a stirred tank are comparable under the selected conditions (Maaß et al. 2009). Please also note the extensive description for the coordinate transformation of the rotating stirrer blade in a vessel into a fixed stirrer blade in the breakage channel in Maaß et al. (2009).

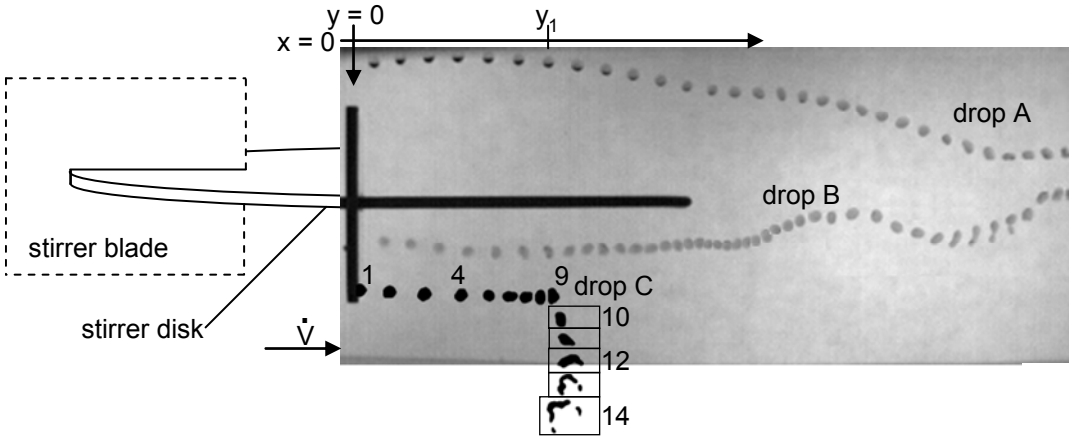

Figure 3 – Three exemplary toluene drops (drop A and B – original images, drop C – after image processing), d_P = 1mm, w = 1.5 m/s, demonstrating the definition of breakage time and breakage probability.

Pictures of the single drop breakage event and the resulting daughter drops are taken with a high-speed camera using a frame rate of 822 fps. Automated image recognition delivers results for the breakage time and number of daughter drops. The different steps of image processing and analysis are described in detail by Maaß et al. (2007). The former software and manual threshold setting is replaced by a full automation in MATLAB®, which uses analysis of the local grey value distribution to determine the right threshold for every sequence. Examples of the high-speed images are shown in Figure 3. Three drops (A, B, C) and their paths through the impeller region are compared with each other. The breaking drop was inserted into Figure 3, after the image processing. Drop C is caught in an eddy which elongates the drop until breakage. From there the drop does not move any further in the y-direction. The expansion of drop images 10 to 14 of drop C displays the breakage process. A more detailed description of Figure 3 follows in the measurement procedure section.

Table 2 – Properties of used chemicals

	γ [mN/m]	γ [mN/m] with dye	ρ [kg/m³] at 20°C	η_d [mPa·s]	c_{dye} [g/L]
toluene	36	32	870	0.55	0.075
petroleum	42	38.5	790	0.65	0.075

The two organic liquids used as dispersed phase for this investigation were toluene (99.98 % purity) and petroleum (99.9 % purity). Both were blended with a non-water soluble black dye, which decreases the interfacial tension between water and the organic liquid but increases the optical evaluation possibilities. The influence on the interfacial tension was quantified using the pendant drop method (Jon et al. 1986). The physical properties for the systems used are listed in Table 2. It is important to mention that petroleum is a mixture and not a pure liquid.

It also has different names; while it is called petroleum in German, it is called kerosene in American English and paraffin oil in British English. Due to the origin of the researcher we will continue to use the term petroleum.

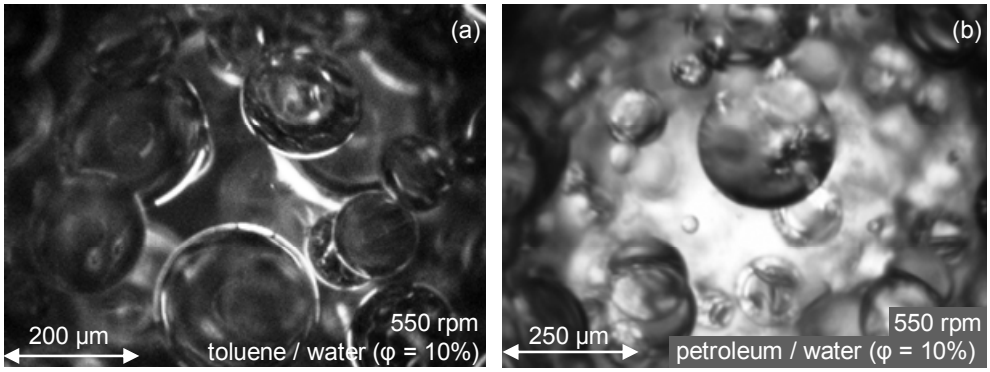

Figure 4 – Example photos of the analyzed systems in a stirred vessel with a Rushton turbine at a stirrer tip velocity of 1.45 m/s.

Experiments in a standard stirred vessel (vessel diameter T = 150 mm, H/T = 1.0) were carried out to determine the influence of the dye on the evolving drop sizes. The photo-optical measurement technique and the experimental set-up that were used are explained in detail by Maaß et al. (2011a). Examples of images of the drops swarms for both systems are given in Figure 4. The distributions with dye were always broader than the ones without. However, the maximum deviation of the Sauter mean diameters ($d_{32} = \Sigma\ d_i^3/\Sigma d_i^2$) with and without dye are less than 10%.

Table 3 – Overview of the working program

system	flow velocity w [m/s]	mother drop diameter d_P [mm]
toluene/ water	1.0	1.0
	1.5	0.67, 1.0, 2.0, 3.0
	2.0	1.0
petroleum/ water	1.0	1.0
	1.5	0.54, 0.7, 1.0, 1.3, 1.9, 3.1
	2.0	1.0

The mother drop sizes have been set between 0.5 and 3.5 mm, which is typical for the larger drops in an agitated liquid-liquid systems (Maaß et al. 2010; Maaß et al. 2011b). A highly accurate dosing pump produces mother drops with standard deviation of the diameter less than 0.003 mm (Maaß et al. 2009). An overview of the whole work program is given in Table

3. The influence of the flow velocity and therewith the energy dissipation rate was varied for a constant mother drop diameter of 1.0 mm. The dependency of the breakage rate on the mother drop diameter was investigated for a constant superficial velocity of 1.5 m/s. The influence of the chemical properties of the systems was shown by parallel investigations with the two used dispersed phases. The viscosity is almost equal to the viscosity of the continuous phase, for both chemicals. So the drop surfaces track the velocity of the continuous phase (Wichterle 1995).

The dimensionless numbers which characterize the application analyzed are given in Table 4 for a 1.0 mm drop diameter. The Reynolds number $Re = w\rho_c D_{\square}/\eta_c$ for all three velocities investigated is significantly above the critical value for turbulent flow. The ratio between the stress exerted on a drop by the flow field and the drop stabilizing pressure exerted by the interfacial tension is called the Weber number We. The definitions according to the applications were given in chapter 2.3. The Weber number displayed in Table 4 is the droplet Weber number. The viscosity ratios in this study are low ($\lambda < 1$). The critical Weber number for such ratios is around one for laminar flow (Walstra 1993) and around 4.5 for pure turbulent flow (Risso and Fabre 1998). Risso and Fabre (1998) even state that for turbulent systems with interfering elongation or shear flow, the critical value for We is below one. All Weber numbers investigated in this study are significantly above the critical values discussed in literature. The shear rate in the thin laminar boundary layer at the impeller blades is not taken into account. The width of this layer can be approximated with $1.8 \cdot 10^{-4}$ m for the slow velocity after Wichterle (1995), and tt is always smaller than the smallest investigated drop diameter in this study. The Ohnesorge number, $Oh = \eta_d/(\rho_d d_p \gamma)^{1/2}$, which characterizes the viscous to interfacial forces, was low for both analyzed materials. When the Ohnesorge number is very small, $Oh < 10^{-2}$, the internal viscous stress is negligible compared to the interfacial stress (Andersson and Andersson 2006).

Table 4 – Overview of the system properties and dimensionless numbers for a drop diameter of 1.0 mm

system	flow velocity w [m/s]	Re [10^3]	Re_{dr} [10^3]	We_{dr} [-]	Ca = We/Re [10^{-3}]	Ca_{dr} = We/Re_{dr} [10^{-2}]	Oh [10^{-3}]
toluene/ water	1.0	22	1.3	16.0	0.74	$1.2 \cdot 10^{-2}$	3.3
	1.5	30	1.8	30.2	1.00	$1.7 \cdot 10^{-2}$	3.3
	2.0	38	2.3	48.9	1.30	$2.2 \cdot 10^{-2}$	3.3
petroleum/ water	1.0	22	1.1	13.3	0.62	$1.2 \cdot 10^{-2}$	3.7
	1.5	30	1.5	25.1	0.85	$1.7 \cdot 10^{-2}$	3.7
	2.0	38	1.9	40.7	1.10	$2.1 \cdot 10^{-2}$	3.7

3.2 Measurement procedure

For statistically firm conclusions, more than 750 events are recorded for one parameter combination (constant drop diameter and flow velocity). These experimental results generate the base for experimentally determined breakage rates after the pioneering equation from Coulaloglou and Tavlarides (1977) (see equation (3)). Although this approach is very time consuming (Vankova et al. 2007), it has the advantage that the breakage results of probability, time and number of drops, formed upon breakage events, are directly determined during observation.

The breakage probability is the relation between the number of all breaking drops and the complete parent population. Three sequences of exemplary toluene drops (d_P = 1.0 mm, w = 1.5 m/s) are shown in Figure 3. The paths of three drops through the breakage channel are presented. Although the boundary conditions are the same, out of the three drops only drop C is breaking. Drop A and B go through the high turbulent region behind the stirrer blade and are deformed by the colliding eddies – drop B is even deformed into a "peanut." The surface forces are always stronger than the inertial forces, though, so the drops always stabilize and remain without breakup. These results are control additionally via a mass balance to gain security.

A comparison of A and B shows that this behavior is not connected to the entrance coordinate. The drops which are not breaking are distributed over the channel entrance coordinate as the complete parent population (details for entrance distribution have been presented by Maaß et al. (2009)). Drop C represents a breaking drop after the image processing. The position of the particle can only be used until y_1. At this point, the drop is caught in a local eddy. All eight of the framed images following remain at the same position and are only moved to represent a whole breakage event in Figure 3. The local eddies are deforming the particles. Thereby, the drops are elongated until they are deformed up to a critical width to break. This moment (represented in Figure 3 with drop image 13) is the time of the first breakage. Here the breakage time t_b is taken. The stirrer blade (y = 0, drop image 1) marks the starting point for the timing of the first breakage. The delta in the images can be directly related to the frame rate. The breakage time for drop C is 0.016 seconds. This definition is in accordance to Janssen and Meijer (1993) and the experimental definition of Risso and Fabre (1998), who investigated the breakage of bubbles under microgravity conditions.

3.3 Parameter estimation

The models for drop breakage rates used in the population balances contain fitting parameters. Traditionally, each author presents his own set of parameter values, based on trial-and-error attempts to reproduce experimental results in liquid-liquid applications (Ribeiro et al. 2011). In this study the fitting parameters are determined based on single drop experiments. The following paragraph describes the parameter estimation procedure for the breakage probability; the procedure for breakage time is similar.

The breakage probabilities are measured for constant process parameters for at least 750 single drops. The average value is calculated from this data set. For statistical evaluation the standard deviation σ is calculated from the development of the average value over the number of single drops that were investigated. The values of the standard deviations for the average breakage probability are always significantly lower than 10%, except for the smallest investigated diameter (11.1%). All absolute values are given together with the experimental results in Table 9 and Table 10 in the appendixes.

The measured values were than compared with model values for the same boundary conditions (energy dissipation rate and physical properties). The model value is fitted against the experimental value by changing $c_{2,b}$ (respectively $c_{1,b}$ for the breakage time). This is done with the mother drop diameter as the control variable. The parameters were fitted not only against one experiment but for all investigated mother drop diameters simultaneously. The sum of the error squares was minimized using the generalized gradient algorithm (Haggag 1981):

$$\sum_{i=1}^{n} \left(x(d_{p,i})_{exp} - x(d_{p,i})_{mod}\right)^2 \rightarrow \min \tag{14}$$

To weight the different experimental results according to their statistical robustness, the error square of each value couple was weighted with the standard deviation. This factor was the square of the difference between one and the standard deviation of the experiment in percent:

$$\sum_{i=1}^{n} \left(\left(x(d_{p,i})_{exp} - x(d_{p,i})_{mod}\right)^2 \cdot \left(1 - \sigma_{i,exp} \Big/ x(d_{p,i})_{exp}\right)^2 \right) \rightarrow \min \tag{15}$$

An experimental value with a low standard deviation is robust and following equation (15) it has a higher impact on the estimation procedure. A value with low confidence has a high standard deviation. Thereby, it has much lower impact on the parameter estimation.

4 RESULTS OF THE SINGLE DROP EXPERIMENTS

In this chapter the experimental single drop results for the breakage probability and the breakage time are presented. The results are discussed and analyzed in detail by a comparison with model approaches from literature.

4.1 Breakage probability

For a given set of system parameters, the breakage probability is defined as the ratio between the number of broken drops and the total number of injected drops of a given size (see equation (3)). The significance of the analyzed data set is always tested by cumulative averaging of the observed results over the number of breakage events. Those results are given in Figure 5. Petroleum and toluene drops are both presented at a constant flow velocity of 1.5 m/s. As a general trend, the breakage probability rises with increasing mother drop diameter, for both analyzed systems. Note that due to the low breakage probabilities of the smallest investigated diameter, the overall number of breakage events investigated was increased to gain enough breaking drops.

The average values of the breakage probabilities with the associated standard deviations are now compared with different model approaches from literature. The results for the petroleum drops are presented in Figure 6. All models shown here follow the general trend of increasing probabilities with increasing mother drop diameter. The parameters $c_{2,b}$ were estimated following the procedure explained in chapter 3.3. The experimental results around the 1.0 mm mother drop diameter are scattered, which makes it harder to find the optimal fitted set of parameters for the models. However, all models reflect the development of the probability for all drop data with satisfying results.

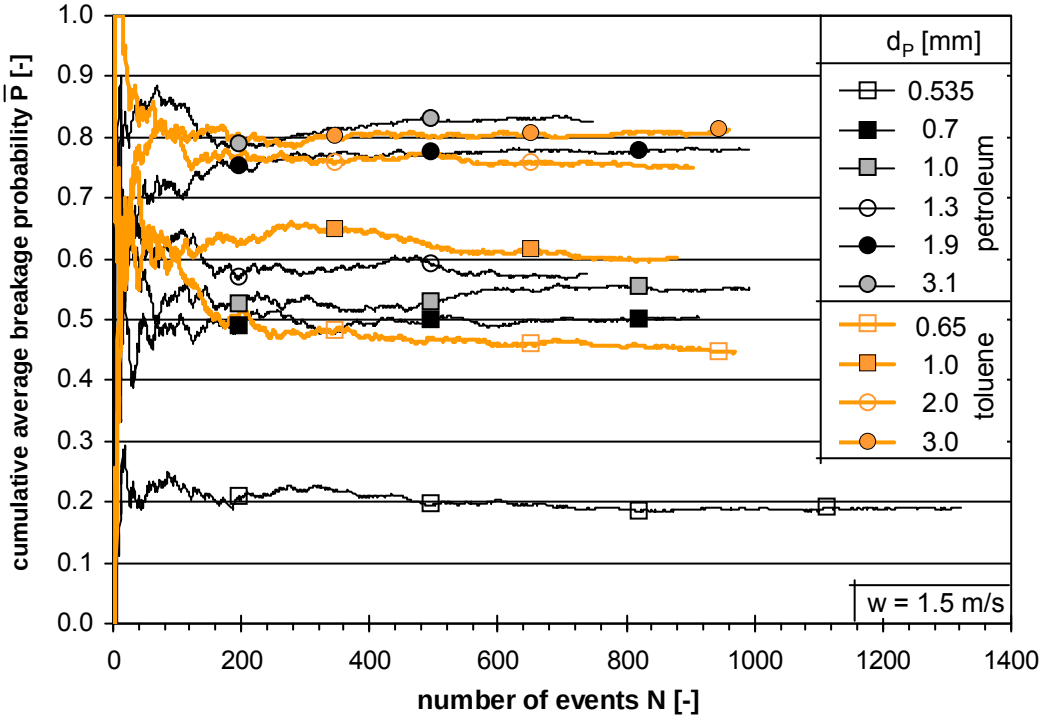

Figure 5 – Cumulative arithmetic average breakage probability as a function of breakage events of toluene and petroleum drops at a constant flow velocity for different mother drop diameters.

The model results gained with fitted values of $c_{2,b}$ are given in Figure 6. Note that the drawback of a second parameter in the model of Chen et al. (1998) was avoided by keeping it constant to the original value. The low value ($7.85 \cdot 10^{-3}$) leads to a negligible viscous force. The breakage probability model is dominated by the surface forces of the petroleum drops. This is a reasonable assumption due to the low viscosities of both the petroleum and toluene drops. The small Ohnesorge numbers (see Table 4) determine already this assumption.

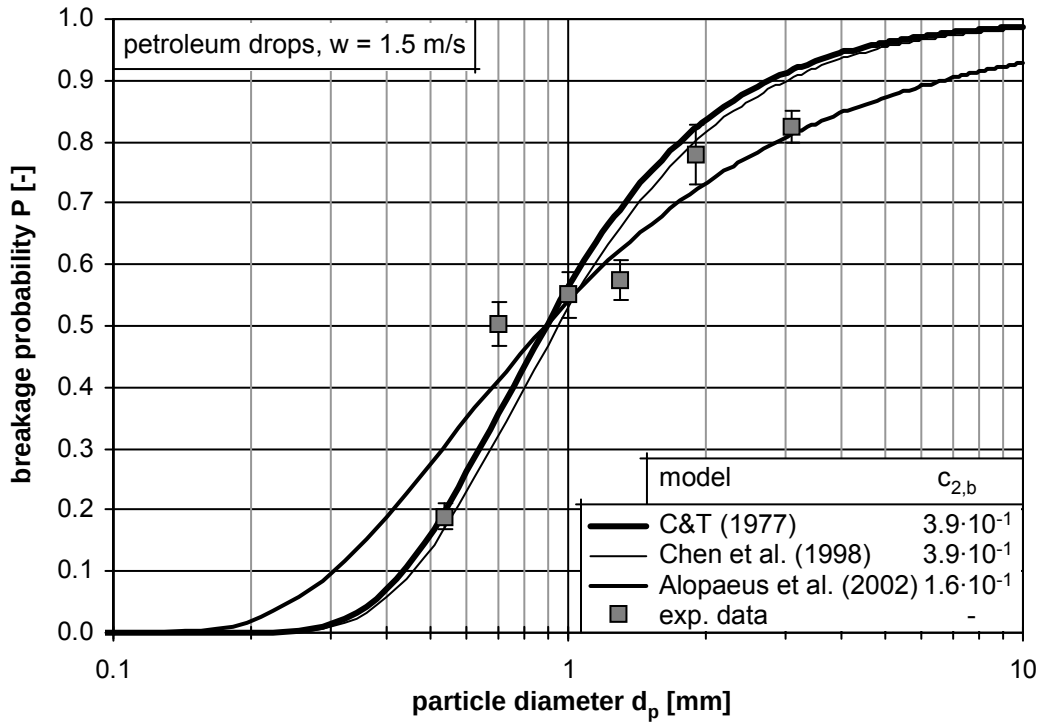

Figure 6 – Comparison of three breakage probability models (lines) with experimental single drop results for petroleum drops (symbols).

Table 5 compares the fitted parameters based on the single drop experiments with those from literature. Therefore, an average value out of several literature sources was calculated. The fitted values of $c_{2,b}$ are in the same order of magnitude for Coulaloglou and Tavlarides (1977). For the model of Chen et al. (1998), the optimum value, based on single drop experiments, is two orders of magnitudes larger than the average value from literature; for Alopaeus et al. (2002) the optimum value is one order of magnitude larger. An overview of all literature sources that were studied, using the presented models, is given at the end of the study (see Table 8 in Appendix A).

Table 5 – Comparison of average breakage probability model parameters from literature with results from single drop experiments in this study (for each single parameter value related to the original source see Table 8 in Appendix A)

model from Coulaloglou and Tavlarides (1977)	in equation (6)
average value $c_{2,b,av}$ from literature	0.69
variance $V(c_{2,b})$	2.00
value $c_{2,b}$ this study	0.39
model from Alopaeus et al. (2002)	in equation (12)
average value $c_{2,b,av}$ from literature	0.031
variance $V(c_{2,b})$	<0.01
value $c_{2,b}$ this study	0.16
model from Chen et al. (1998)	in equation (9)
average value $c_{2,b,av}$ from literature	0.003
variance $V(c_{2,b})$	< 0.01
value $c_{2,b}$ this study	0.39

In Figure 7 the chosen parameters are tested for the toluene probability results. The deviations between the experimental results and the model approaches by Coulaloglou and Tavlarides (1977) and Chen et al. (1998) are increasing with changing the dispersed phase system. In contrast, the model of Alopaeus et al. (2002) perfectly predicts the experimental number of breaking drops for the investigated time interval. Due to the chosen parameters and thereby the subordinate role of the viscous forces, the structure of equation (12) is equal to the original model proposed by Narsimhan et al. (1979). A broader variation of the dispersed phase viscosity is necessary to determine its influence. Based on the satisfying results, we will consider the erfc-term from equation (12) from Alopaeus et al. (2002) as a robust probabilistic model approach which describes the ratio between breaking and total number of drops satisfying for the two investigated cases.

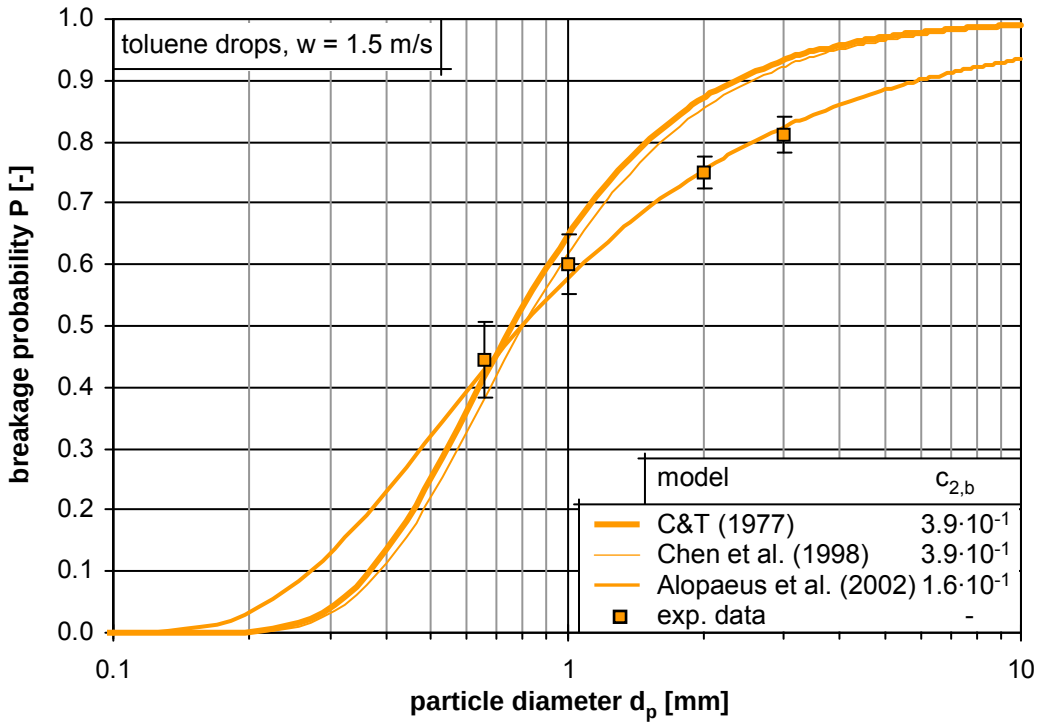

Figure 7 – Comparison of three breakage probability models (lines) with experimental single drop results for toluene drops (symbols).

4.2 Breakage time

The discussion about the breakage time is much more controversial than the discussion about the breakage probability. Most of the contradicting opinions published were already presented in chapter 2.2. These theories will be evaluated with single drop experiments. Figure 8 presents the significance of the achieved experimental breakage times by cumulating the arithmetic average breakage time $t_{b,av}$ over the number of investigated events. All data sets run into a constant average value.

A general trend is hard to define when analyzing these average values (see also the table in Figure 8). Three main theses can be pointed out: Firstly, the highest value of the breakage time for petroleum and toluene is always connected to the smallest mother drop diameter. Secondly, the average breakage time $t_{b,av}$ seems to have a minimum for a certain mother drop diameter. Thirdly, $t_{b,av}$ of the toluene drops for a chosen diameter is always lower than for the petroleum drops with a comparable diameter. All those results have been achieved for a constant superficial velocity of 1.5 m/s. The average energy dissipation rate was constant for all experiments.

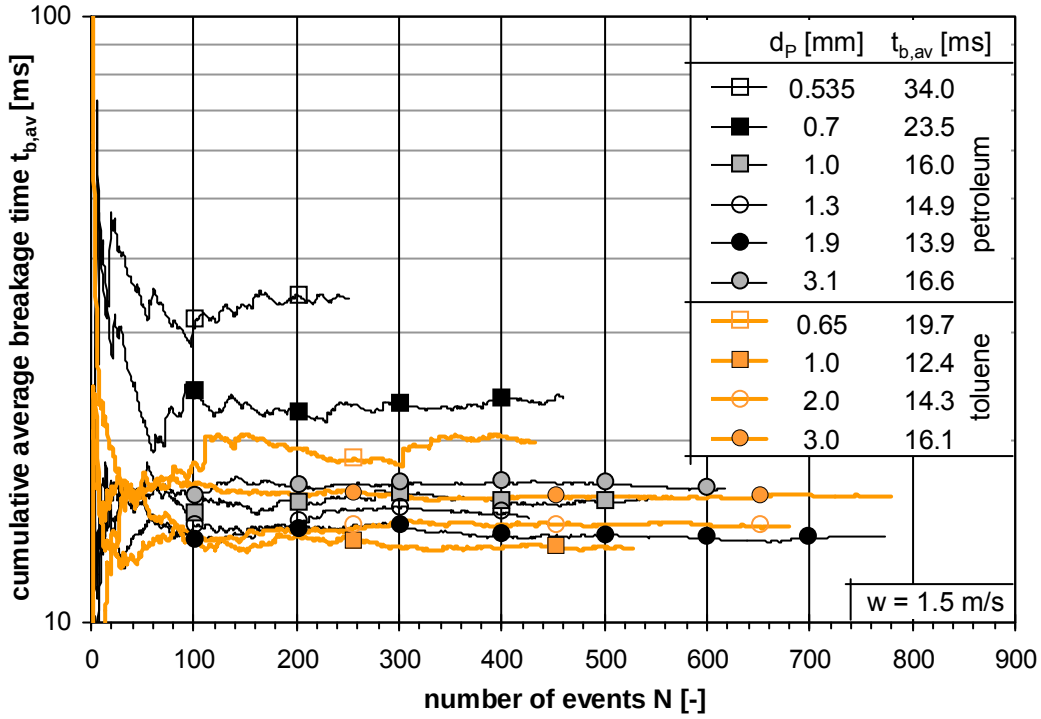

Figure 8 – Cumulative arithmetic average breakage times as a function of analyzed breakage events for a constant flow velocity and various mother drop diameters.

For a more detailed differentiation, the relative numbers of distributions of the breakage time are analyzed. Therefore, the breakage time distributions corresponding to the highest and the lowest average value for petroleum drops are compared at a constant flow velocity of 1.5 m/s in Figure 9. The distributions are not following a normal or a log-normal distribution around the arithmetic average values ($t_{b,av}$ are displayed by the orthogonal dotted lines in Figure 9). A β-distribution was a very good fit for all experimental distributions (straight lines), which reflects the unequal distribution of the number of events over the breakage time. The distribution of the larger mother drops is more equal than for the smaller drop. This can be measured by the difference of the maximum value of the β-distribution and the arithmetic average value. This difference is 31.3 ms for the 0.535 mm and only 4.0 ms for the 1.9 mm drops.

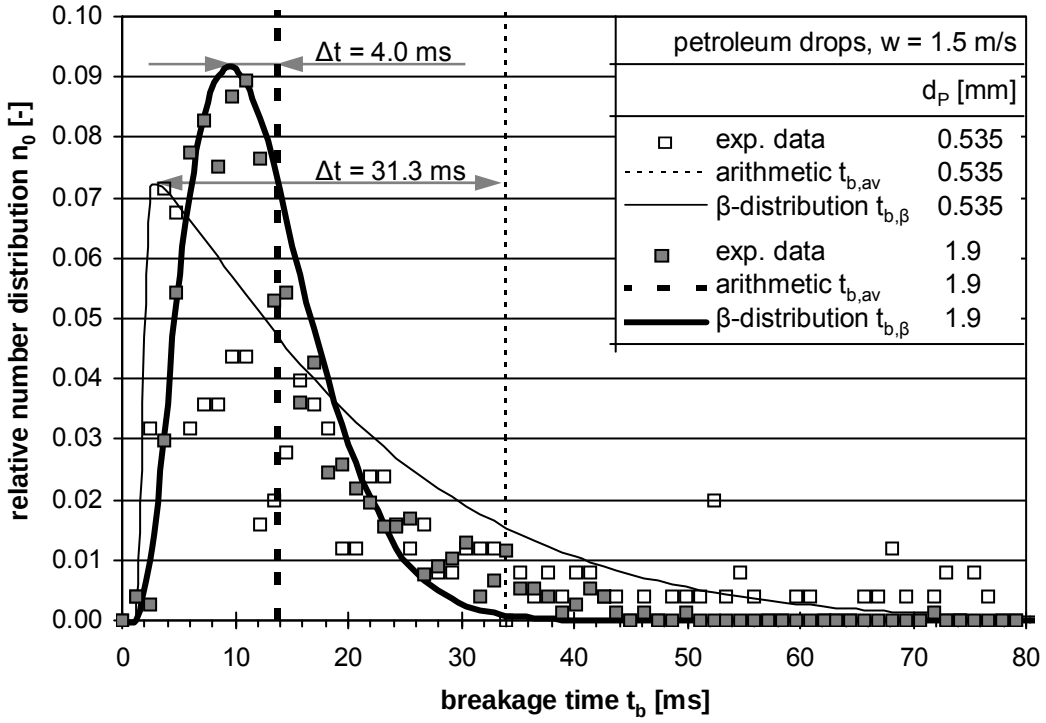

Figure 9 – Relative number distribution of the breakage time (symbols) and its approximation with a β-distribution (lines) for two different petroleum mother drops at a constant flow velocity.

The small particles can circulate a particularly long time in the turbulent region behind the stirrer blade, until they break. Figure 10 illustrates the phenomena with five example drops. Part (I) of Figure 10 shows the path and the breakage time of three equally-sized mother drops at a constant flow velocity of 1.5 m/s. Drop A is breaking on the second image due to the collision with the stirrer blade. Drop B is breaking after 75.4 ms, which is almost double the length of the average residence time ($t_{res} = \dot{V}/V_r$, with $V_r = 30x30x70\ mm^3$) for the presented flow velocity. Even more extreme is the path and breakage time of drop C. The drop is caught in a large eddy behind the blade, transported back against the flow direction for more than 50 ms, caught again in a smaller eddy and than finally breaking after 141.1 ms, which is equal to 116 images. These three drops show the whole recorded breakage time spectrum for the 1 mm mother drop.

Part (II) illustrates the breakage time of two different-sized mother drops. While drops are only broken by eddies equal and smaller their size (Shinnar 1961), the 0.7 mm drop (drop D) is breaking after it circulated more than 300 ms. In contrast, the 1.9 mm drop is breaking directly at the stirrer blade.

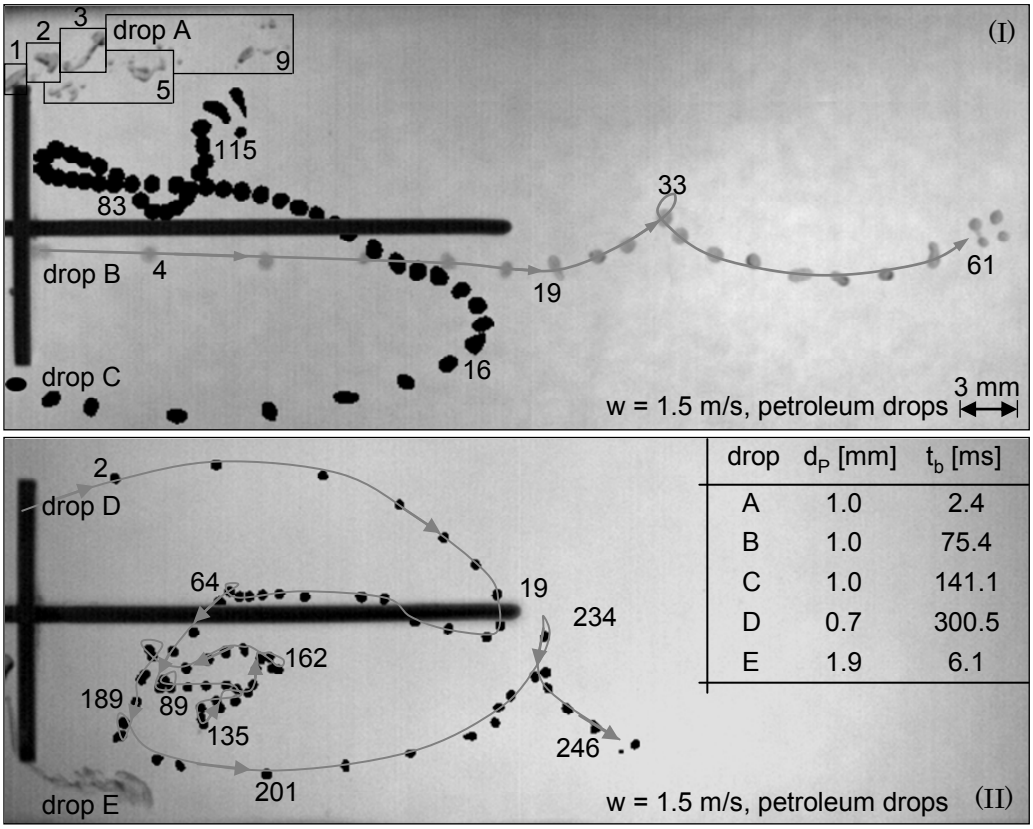

Figure 10 – Example high-speed images (original – drop A,B,E and after image processing – drop C,D) to illustrate the differences in the breakage time for a constant stirrer speed and a varying mother drop diameter.

The probability of a higher circulation time is increasing with decreasing drop size. The total number of larger eddies which are able to catch a drop and transport it rather than break it is increasing with decreasing drop size. This stochastic phenomenon is already implemented in the breakage probability and displayed by lower values of the breakage probability for smaller particles than for large ones. However, the equal consideration of these extreme long breakage times leads to a strong increase of the average value, but mainly for the smaller particles. The comparisons of the peak values of the β-distributions are much easier to interpret than the average values.

Figure 11 shows the experimental results of the breakage time for increasing petroleum mother drops at a constant flow velocity of 1.5 m/s. The average of the peak values of the β-distributions are compared with model values. The average values $t_{b,av}$ (circles) are decreasing to a certain diameter and increasing again. The peak values of the β-distribution $t_{b,\beta}$ (squares) are monotonically increasing. The trend of $t_{b,\beta}$ seems much more reasonable to the authors than the trend of the simple average values. Note that for the 3.1 mm drops, both interpretations already lead to the same result. This supports the assumption that only the circulation time of smaller drops misleads the interpretation of the arithmetic average values. However, the experimental results from literature (given in Table 1) are in good agreement with the

results achieved in this study. Independent from the used experimental set-up, the breakage times reported in literature vary from 3.4 to 100 ms.

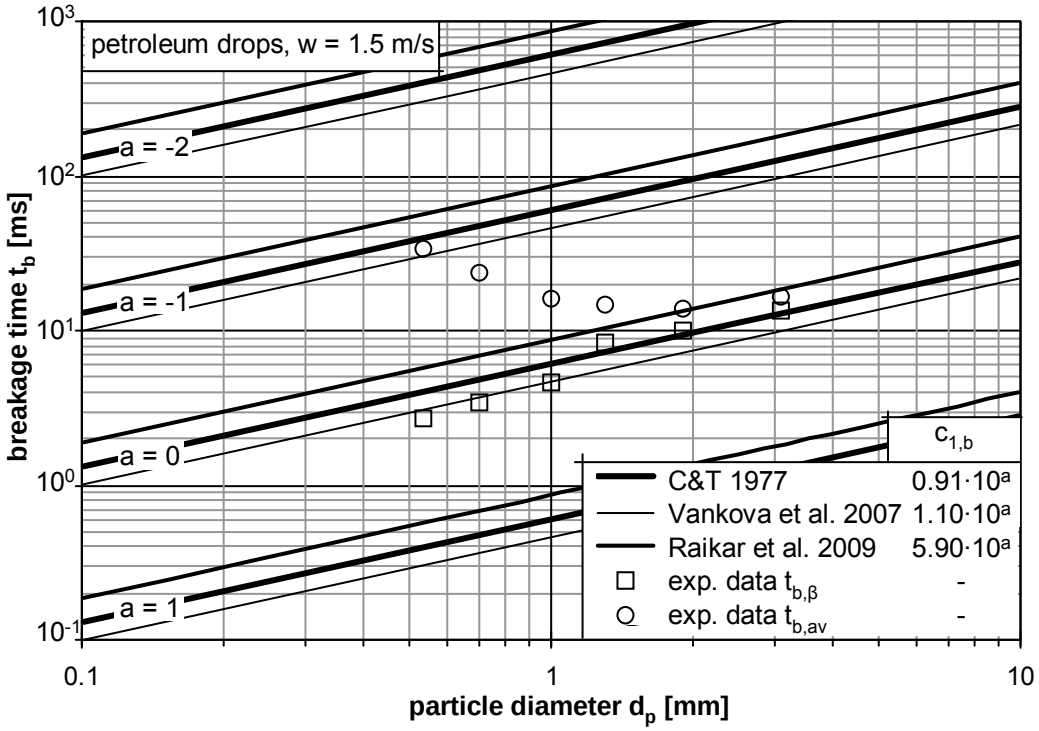

Figure 11 – Comparison of three breakage time models at different parameter magnitudes (lines) with experimental single petroleum drop results (symbols).

The comparisons with literature models shows clearly that earlier assumptions – like the one from Chen et al. (1998) that t_b is a constant value – can be considered erroneous. All models presented in Figure 11 propose a dependency of t_b on $(d_P)^{2/3}$ and so they display the development of the $t_{b,\beta}$-values. With adaptation of the constants in the models, all are able to predict the development of the breakage time very well. The $c_{1,b}$-values reported in literature create breakage times one or even more magnitudes larger than the experimental ones. The optimized value of $c_{1,b}$ for the model of Coulaloglou and Tavlarides (1977) is one magnitude higher than the highest value reported in literature (see Table 8 for a short parameter overview from literature in Appendix A). Breakage and coalescence terms influence each other so that different mathematical solutions are possible to display one set of experiments. Ribeiro et al. (2011) even propose that the interdependence between the kinetics of coalescence and breakage processes leads to a constant ratio between the coalescence and breakage parameters.

To avoid a local optimum, physical interpretation of the parameter magnitude is necessary. The lowest values reported in literature by Gäbler et al. (2006) are three magnitudes smaller than the values found here. Subsequently, their breakage time is three magnitudes higher than the observed one in this study. The authors are aware of the high challenges in parameter fitting for population balance equation, but we propose to compare the results of the parameter optimizations with the physical meaning of the optimized kernel. A value of $c_{1,b} = 10^{-4}$

leads to a breakage time for a 3.0 mm toluene drop of around 100 s at the investigated flow velocity of 1.5 m/s. This should be questioned and compared to the physical application of the simulation.

In Table 6, available average values for parameters used in the literature are compared with the optimized parameters based on the single drop experiments. The large number of available parameter results of the model from Coulaloglou and Tavlarides (1977) and their relatively low spreading show a clear tendency. Opposed to the experimental results in this and former studies (see Table 1), the modeled breakage times are one to two magnitudes higher than the experimental results.

Table 6 – Comparison of average breakage time model parameters from literature with results of $t_{b,\beta}$ from single drop experiments in this study (for each single parameter value related to the original source see Table 8 in Appendix A)

model from Coulaloglou and Tavlarides (1977)	in equation (5)
average value $c_{1,b,av}$ from literature	0.18
variance $V(c_{1,b})$	0.11
value $c_{1,b}$ this study	0.91
model from Vankova et al. (2007)	in equation (7)
value from $c_{1,b}$ Vankova et al. (2007)	0.033
value $c_{1,b}$ this study	0.82

This discrepancy is the same for the toluene values presented in Figure 12. The previously mentioned petroleum results are compared with the ones observed from the toluene drops. Only the peak values from the β-distributions and the associated standard deviations are used for the comparison. All absolute values for both kinds of breakage times (arithmetic average and peak value from β-distribution + standard deviations) are given in Table 10 - Appendix . While the model of Coulaloglou and Tavlarides (1977) and Chen et al. (1998) do not display the influence of physical properties on the breakage time, the same plots have to be used for both systems. As discussed in chapter 2.2, Vankova et al. (2007) and also Raikar et al. (2009) extended the traditional form from Coulaloglou and Tavlarides (1977) to take physical changes of the system into account. A comparison of equations (7) and equation (8) shows that both extensions propose an increasing breakage time with increasing dispersed density. These results are given in Figure 12 as line III. Due to the same proportionality of both models between t and ρ_d, their results fall to the same curve. The prediction is opposed to the experimental results. Without further improvements, we can not consider these approaches any further in this study. The optimized parameters of $c_{1,b}$ are given in addition in Figure 12 (see also Table 6).

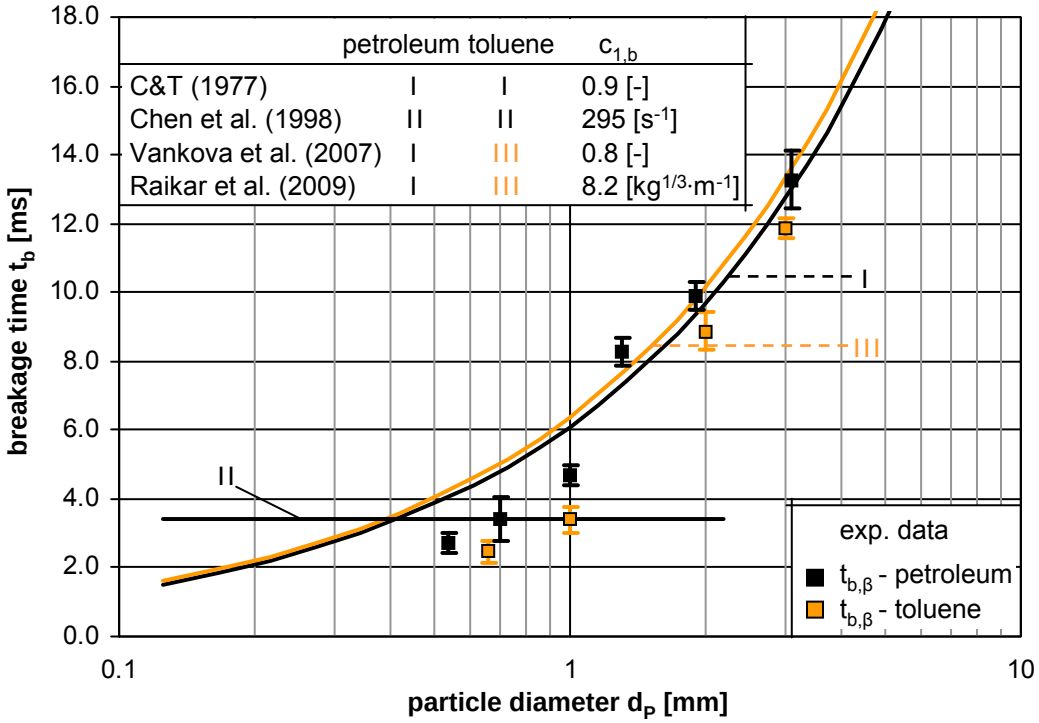

Figure 12 – Comparison of four breakage time models at a constant superficial velocity of 1.5 m/s (lines) with experimental single toluene and petroleum drops (symbols).

The influence of the energy dissipation rate ε and thereby the flow velocity is analyzed in Figure 13. The used ε values are local values comparable to a stirrer region with the size from the breakage channel. The transformation was shown by Maaß et al. (2007).

The rise of the flow velocity increases the turbulence, its fluctuation velocities and the energy of the turbulent eddies. The drops are breaking easier and faster. This is true for the average value as for the peak value of the corresponding β-distribution. The dependency of t_b on $\varepsilon^{-1/3}$, derived from turbulence theory (Coulaloglou and Tavlarides 1977) could be shown for the average values as for the peak values of the breakage time. This dependency was already introduced in most of the model approaches. The model of Chen et al. (1998) neglects this dependency.

The results of the breakage time show that the experimental results in this study and in theory are in accordance to each other. Again, the magnitude of the experimental results is smaller than the one from literature models. The influence of the dispersed phase is not or only poorly reflected in all models. The dependency of the single drop experimental breakage times on the energy dissipation rate is in accordance with the dependency of t_b on ε in literature models.

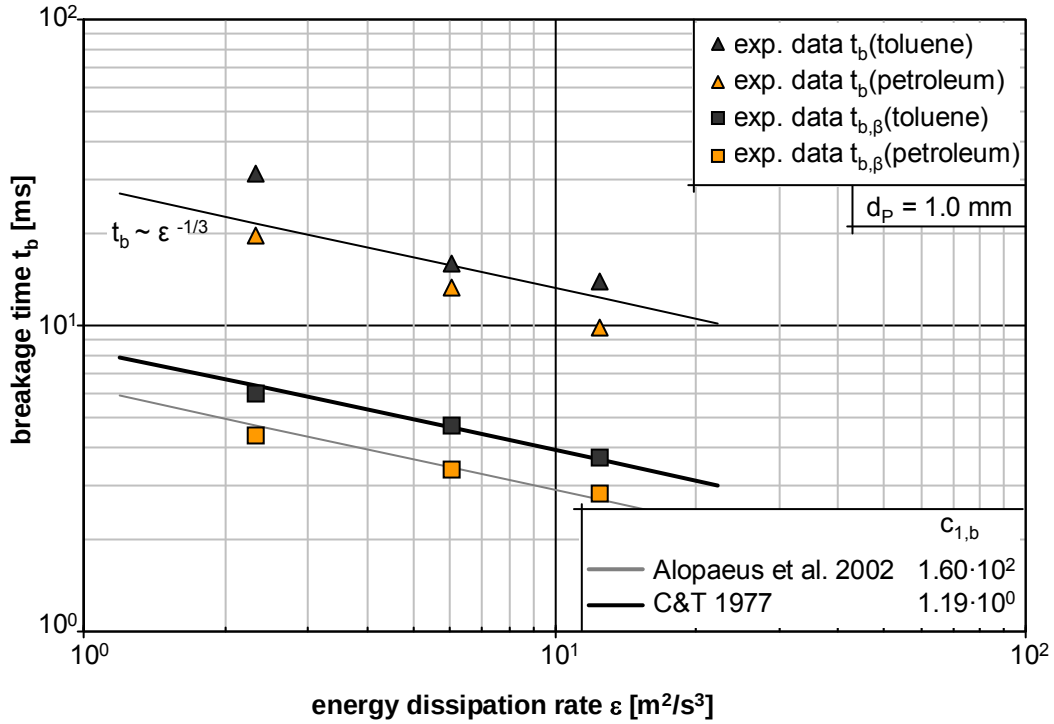

Figure 13 – Dependency of the breakage time on the energy dissipation rate, experimental and model results

5 A NEW MODEL APPROACH FOR THE BREAKAGE TIME

The modeling of the breakage time has the highest optimization potential based on the results in chapter 4.1 and 0. In this chapter we want to include different breakage mechanisms into the correlation of the breakage time. Therefore, we will connect breakage times based on the turbulent pressure fluctuation (see equation (5)) with those induced by the two-dimensional (2D) elongational flow field in front of the rotating blade. We consider these mechanisms operating simultaneously. The elongations of drops by accelerating rates (Stoots and Calabrese 1995) close to the blade are not considered in the description of the breakage time.

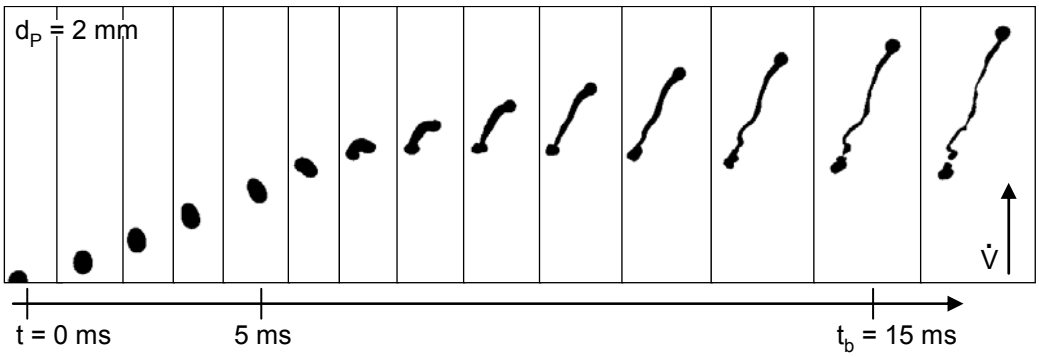

Figure 14 – Example of a breakage event based on drop elongation in the turbulent flow

The experimental results clearly showed that drop elongation plays an essential role in the breakage processes. An example of such an elongation-induced breakage event was displayed in Figure 14. A 2.0 mm toluene drop was entering the turbulent region behind the stirrer blade. Not the microscopic turbulent fluctuations, but the macroscopic accelerations, by the flow are deforming the drop. As it approached the tip region, the drop accelerated and experienced stretching before breaking. The main idea of the breakage process at constant stretching rate was illustrated by Janssen and Meijer (1993). They assumed that for 3D elongational flows, the orientation of the extending thread is permanently aligned with the principal axis of strain and $\dot{\varepsilon}$ is the classic rate of elongation. This constant elongation leads to a thinning of the liquid thread as exemplary shown in Figure 14. With the initial diameter $d_{P,0}$ this process can be described over time in form of an exponential interrelation.

$$d_P(t) = d_{p,0} \exp\left(\frac{-\dot{\varepsilon} t}{2}\right) \tag{16}$$

This equation can be transformed into a description of the thinning process time t as a function of the thinning diameter d_P. Due to the physical root of the thinning process, this time will be called elongation time t_e as a function of the elongated particle diameter $d_{P,e}$:

$$t_e = \frac{2}{\dot{\varepsilon}} \ln\left(\frac{d_{P,0}}{d_{P,e}}\right) \tag{17}$$

Figure 15 shows the development of this elongation time as a function of different elongation rates. The initial size for the example drop in this figure is 1.0 mm. Obviously, higher elongation rates are leading to smaller elongation times for the same thinning of a certain drop.

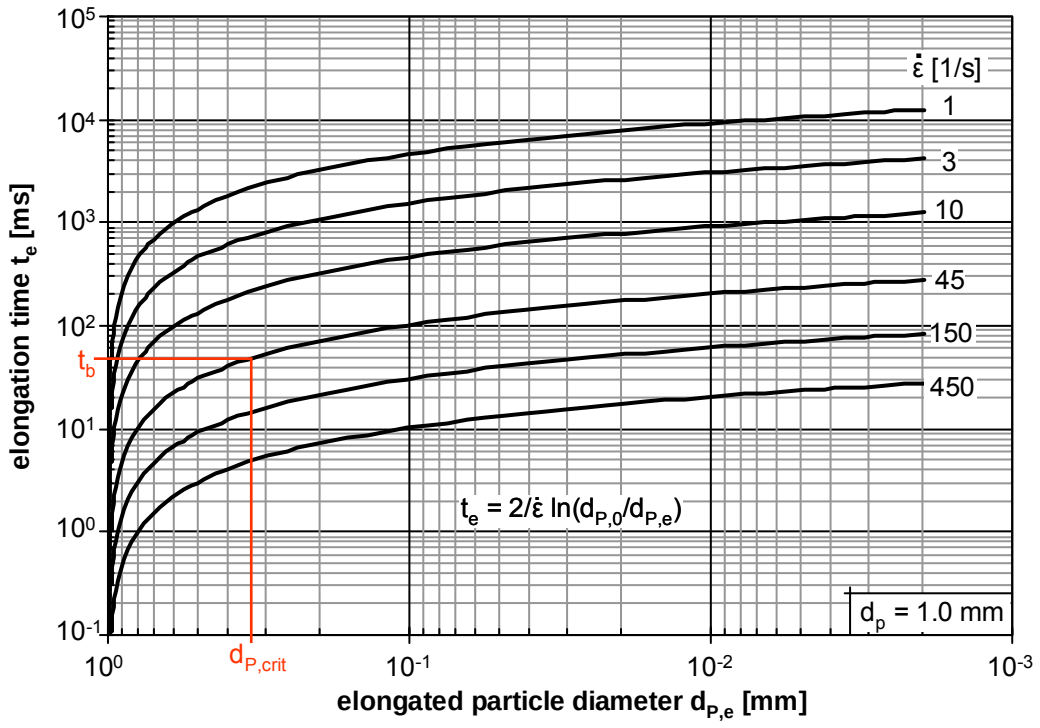

Figure 15 – Development of the elongation time over the thinning fluid particle thread as a function of the elongation rate $\dot{\varepsilon}$

An arbitrary critical diameter is exemplarily introduced in Figure 15. This diameter describes the critical thickness of the elongated thread, at the point where the thread will break. From Figure 15 it can easily be seen that with the knowledge of the critical diameter $d_{P,crit}$ and the elongation rate $\dot{\varepsilon}$ the breakage time t_b can be determined. Therefore, a breakage time based on the elongation can be derived:

$$t_{b,e} = \frac{2}{\dot{\varepsilon}} \ln\left(\frac{d_{P,0}}{d_{P,crit}}\right) \tag{18}$$

Former results of experimental studies involving elongational fields have been summarized by plots of the Capillary number, against the ratio of the viscosities of the dispersed and continuous fluids. These plots provide an indication of the critical Capillary number, Ca_{cr} , that governs the stability of a drop in the straining field and depends on the type of flow; drop breakup occurs for $Ca > Ca_{cr}$ (Mietus et al. 2002).

In equation (19) the drop Capillary number that puts the viscous forces of the drop under elongation with the capillary forces in interrelation is shown.

$$Ca_{dr,e} = \frac{\eta_d w}{\gamma} \tag{19}$$

The characteristic velocity in this equation can be described by the deformation rate:

$$w = \dot{\varepsilon} \cdot d_{P,crit} \tag{20}$$

This description allows the forming of equation (21), which gives the definition for the critical thread diameter of the elongated drop as a function of the elongation rate and the physical properties of the investigated media.

$$d_{P,crit} = \frac{Ca_{dr,e,crit} \cdot \gamma}{\eta_d \cdot \dot{\varepsilon}} \tag{21}$$

With the combination of equation (17) and (21), we can derive a formulation of the elongation induced breakage time $t_{b,e}$:

$$t_{b,e} = \frac{2}{\dot{\varepsilon}} \ln\left(\frac{d_{P,0} \cdot \dot{\varepsilon} \cdot \eta_d}{\gamma \cdot Ca_{dr,e,crit}}\right) \tag{22}$$

Note that for a critical diameter larger than the initial diameter, the expression becomes negative. Therefore, a boundary condition was set that $t_{b,e}$ becomes infinity for droplets smaller than the critical thread diameter. Certain drop sizes can therefore not be broken by the elongation. If the elongation breakage time is equal to infinity than the elongation-based breakage rate is zero.

Equation (22) contains two unknown parameters: the elongation rate and the critical Capillary number of the elongated drop. Determination of the elongation rate will require an analysis of the three-dimensional flow. In principle, this can be obtained by solving the equations of motion for both the drop and fluid medium with free boundary, but in practice, the approach is very complex. Since our interest in this analysis is only to estimate the magnitudes of the elongation rate in the zone of highest stretching, we will use the values presented by Stoots and Calabrese (1995) for the elongation rate close to a Rushton turbine.

The values for critical Capillary numbers in such irregular 3D flow are not reported in detail in literature yet. Mietus et al. (2004) mentioned that the deformation and breakup of a drop during complex mixing processes should rather be based on local Capillary numbers than on those for the whole system. However, a simplification of the 3D flow into a 2D flow is assumed here, due to the permanent alignment of orientation of the extending thread with the principal axis of strain. Values for the critical Capillary numbers in 2D elongation flows have been reported by Kumar et al. (1998). These and other results show clearly that elongational flow is more efficient in breaking up drops, especially at a high viscosity ratio. This efficiency can only be used for the breaking process if the velocity gradient lasts long enough; the latter may be a problem since in most situations elongational flow is a transient phenomenon (Walstra 1993). Therefore, we propose to set $t_{b,e}$ in relation to the residence time t_{res} of the fluid in the stirrer region with the high elongation rates. An elegant proportionality between the residence time and the stirrer speed was derived by Kumar et al. (1998):

$$t_{res} \propto \frac{1}{18\pi n} = \frac{c_1}{n} \tag{23}$$

The ratio between $t_{b,e}$ and t_{res} is now combined with the turbulent breakage time $t_{b,turb}$ (equation (5)).

$$t_b = \frac{t_{b,e}}{t_{res}} t_{b,turb} \propto \frac{t_{b,e}}{t_{res}} \frac{d_P^{2/3}}{\varepsilon^{1/3}} \tag{24}$$

Assuming that the elongation-induced breakage time is shorter than t_{res}, the breakage time after equation (5) is decreasing. For the opposite case, due to very short residence times, the ratio of the elongation-based breakage time to the residence time is set to one. For such cases, only the turbulent breakage time is relevant for the breakage process. The new model for the breakage time t_b is proposed as follows:

$$t_b = c_{1,b} \frac{n}{\dot{\varepsilon}} \ln\left(\frac{d_P \cdot \dot{\varepsilon} \cdot \eta_d}{\gamma \cdot Ca_{dr,e,crit}} \right) \frac{d_P^{2/3}}{\varepsilon^{1/3}} \tag{25}$$

The experimental results of the single drops have been used to determine an optimum value for $c_{1,b}$ in equation (25). The estimation procedure was the same as described in a previous chapter. The obtained value was 0.18.

Based on the results of the breakage probability and the breakage time, the breakage rate can be calculated and compared with the experimental data from the single drop experiments. The

comparison with theoretical models in the following chapter will lead to a clear judgment about the advantages and disadvantages of the different models based on the experimental study.

6 BREAKAGE RATE RESULTS

The breakage rate or breakage frequency is the most complex modeling approach in the breakage kernel within the PBE (see equation (2)). The broad discussions about drop breakage mechanisms have led to several contradicting models. No standard model could be defined already. In this study we want to achieve a clear statement about the qualitative development of the breakage rate over the parent diameter. Furthermore, we want to validate the different models concerning their prediction quality if physical properties are changed. Due to the limited range of variation, using petroleum and toluene drops, this validation can only be a first hint and needs to be extended in further studies.

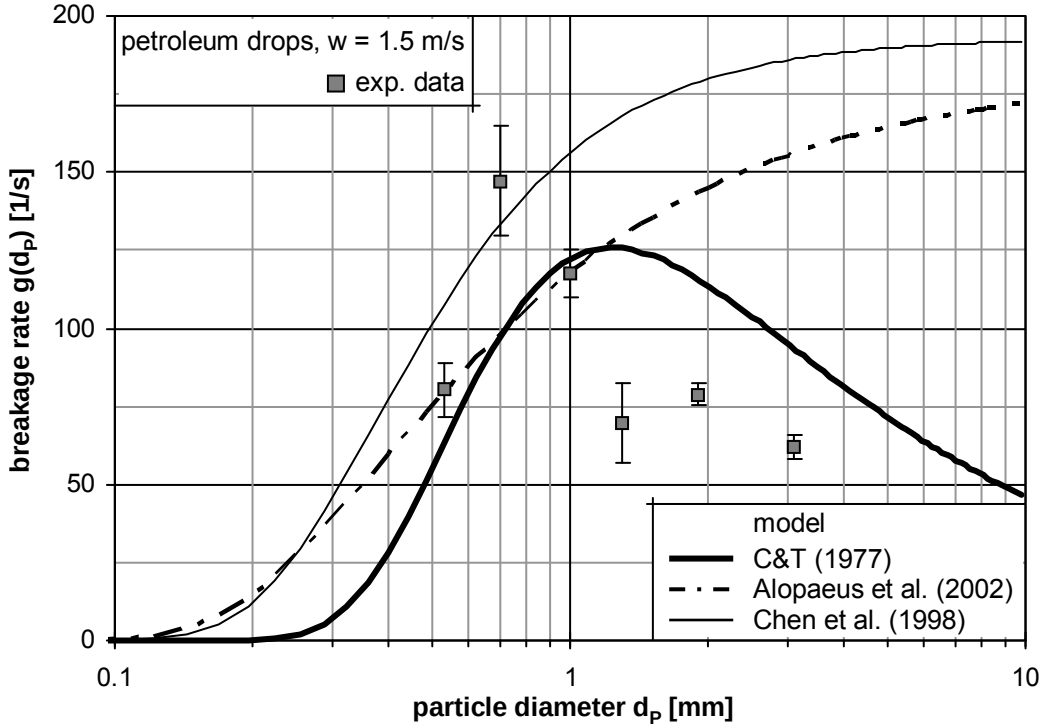

Figure 16 – Comparison of different breakage rates with experimental petroleum single drop experiments, the used parameters in the models are all given in Table 8 in Appendix A (as this study)

The comparison of experimental and theoretical breakage rates is given in Figure 16, at a constant flow velocity of 1.5 m/s, for the petroleum/water system. The used parameters in the models are the optimized values based on the breakage probability and the breakage time in the previous chapters. The overview of the values is presented in Table 8 in Appendix A, declared as "this study." The experimental data clearly shows a maximum for the breakage rate around 0.7 mm due to the strong decrease of the inverse breakage time for increasing

mother drop diameter. Monotone models like the ones by Chen et al. (1998) or Alopaeus et al. (2002) are not able to predict that behavior. The model from Coulaloglou and Tavlarides (1977) qualitatively displays the experimental development, but no unique pair of parameter values is able to predict the complete result range in a quantitatively satisfying matter.

For further discussions, only the breakage rate from Coulaloglou and Tavlarides (1977) developing a maximum for a certain diameter will be taken into account. The comparison between the toluene and the petroleum system is shown in Figure 17. As a general trend, the model and the experiments show higher values for toluene than for petroleum at a given drop size. This increase by changing the physical system is only qualitatively well-described by the presented model. The experimental results show a narrow maximum peak and high gradients on both sides of the maximum. Furthermore the model shows a maximum value too low for the toluene drops, while it is in the right magnitude for the petroleum drops. This could be optimized by an additional fitting of the parameters, which shows the need for a further improvement of the model. The magnitude of the parameter results achieved in this study show similar results to those in literature for the breakage probability ($c_{2,b}$) and are always larger for the breakage time ($c_{1,b}$). Larger values for both parameters, using the model of Coulaloglou and Tavlarides (1977), have only been reported just recently in the work of Azizi and Taweel (2011).

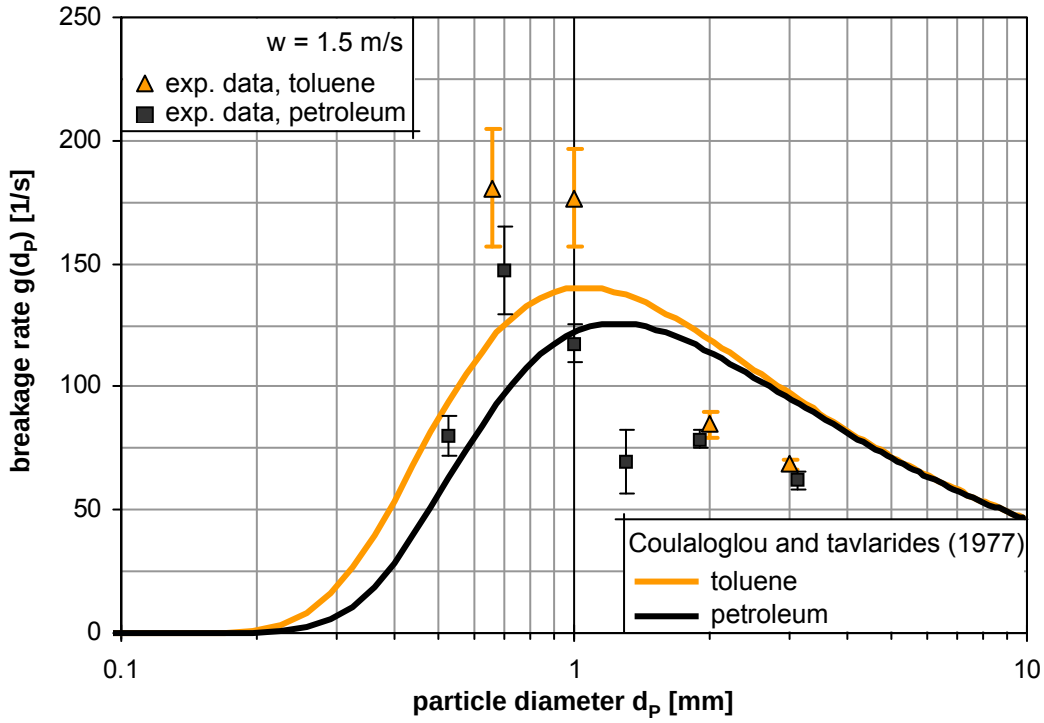

Figure 17 – Comparison of different breakage rates with experimental toluene and petroleum single drop experiments, the used parameters in the models are all given in Table 8 in Appendix A (as this study)

As presented in the previous chapter, a new model for the breakage time was derived. This will be combined with two different breakage probabilities. The first combination is between equation (12), the approach by Alopaeus et al 2002 and equation (25):

$$g(d_p) = c_{1,b}\frac{\dot{\varepsilon}}{n}\left(\ln\frac{d_P\dot{\varepsilon}\eta_d}{\gamma Ca_{dr,e,crit}}\right)^{-1}\frac{\varepsilon^{1/3}}{d_P^{2/3}}\cdot\operatorname{erfc}\left(\sqrt{\frac{c_{2,b}\gamma}{\rho_c d_P^{5/3}\varepsilon^{2/3}}+\frac{c_{3,b}\eta_d}{\sqrt{\rho_c\rho_d}\,d_P^{4/3}\varepsilon^{1/3}}}\right) \tag{26}$$

In the second combination the breakage probability from Coulaloglou and Tavlarides (1977) in its extended form by Chen et al. (1998), presented in equation (9) is used with equation (25):

$$g(d_p) = c_{1,b}\frac{\dot{\varepsilon}}{n}\left(\ln\frac{d_P\dot{\varepsilon}\eta_d}{\gamma Ca_{dr,e,crit}}\right)^{-1}\frac{\varepsilon^{1/3}}{d_P^{2/3}}\exp\left(-\frac{c_{2,b}\gamma(1+\varphi_d)^2}{\rho_d\,\varepsilon^{2/3}d_P^{5/3}}-\frac{c_{3,b}\eta_d}{\rho_d d_P^{4/3}\varepsilon^{1/3}}\right) \tag{27}$$

The exponential term derived by Chen et al. (1998) was an advancement of the breakage probability by Coulaloglou and Tavlarides (1977). This model takes the viscous forces into account. As the variation of viscosity was low in this study, the breakage probabilities of both models are almost equal for the same conditions (see also Figure 6).

The new models of the breakage rate are compared with the experimental results from the single drop experiments in Figure 18. The combination of the newly developed breakage time and the breakage probability of Chen et al. (1998) showed very good agreements with the experimental results. The model not only follows the development of the breakage rate over the particle diameter for both investigated systems, but also is in the right order of magnitudes. The used parameters for the presentation in Figure 18 are presented in Table 7.

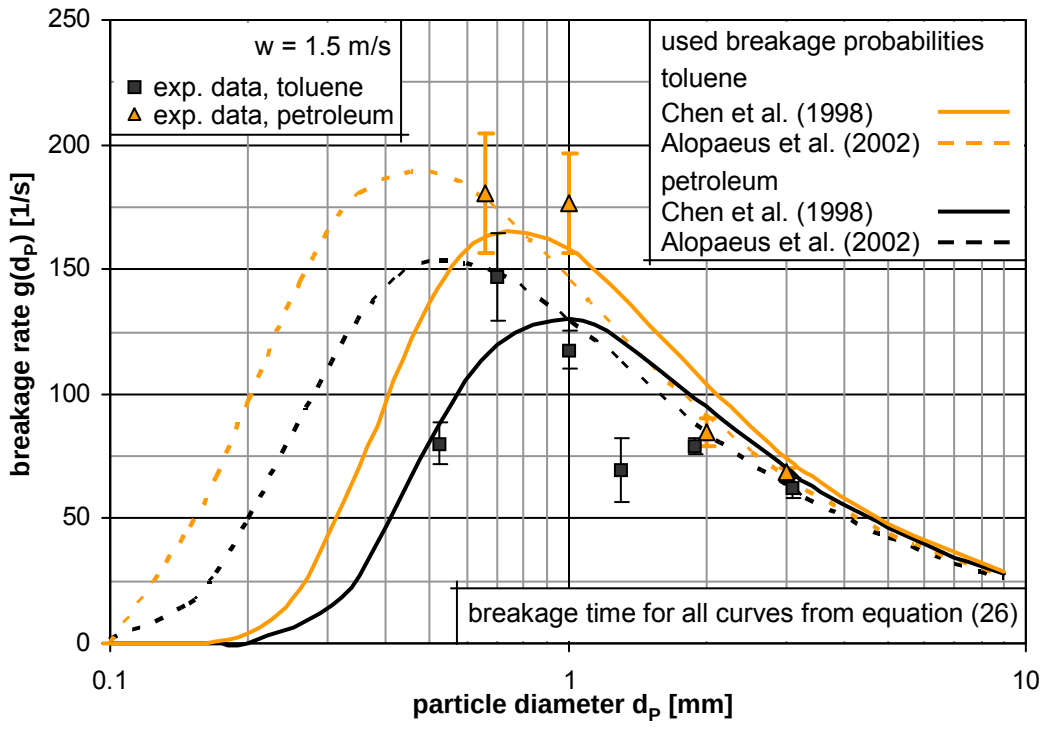

Figure 18 – A comparison of model data (lines) and experimental results (symbols) is shown. The model consists of breakage probability functions from the literature and the new model approach of the breakage time.

The used mixed model with the breakage probability of Alopaeus et al. (2002) predicts high values for the breakage rate of small particles as the distribution of the breakage rate is broader than the other. The predicted value for the smallest particle diameter, which is still breaking, seems too low. However, both mixed model approaches are promising and should be tested in further single drop studies with different physical systems as in simulations of agitated liquid-liquid dispersions.

Table 7 – used parameters for the mixed model approaches from equation (26) and (27)

Model	$c_{1,b}$ [-]	$c_{2,b}$ [-]	$c_{3,b}$ [-]
own model	0.1	-	-
Chen et al. 1998	-	0.39	0.0078 (as original source)
Alopaeus et al. 2002	-	0.16	0.2 (as original source)

7 SUMMARY

In this study, detailed and precise parameter determination for the PBE models of the breakage rates have been carried out in a single drop breakage cell. The breakage rate is the product of the inverse breakage time and the breakage probability. Those two physical data have been collected for numerous single toluene and petroleum drops, using high-speed imaging. Literature models have been compared with the results of the single drop experiments. Several literature approaches of the breakage probability showed good agreements with the experimental data. The magnitude of the probability, defined by the used model constants, is in good agreement with the single drop experiments.

The comparison of model approaches for the breakage time and the single drop results are contrary. On one hand the model approaches contradict each other in their description of the influence of the particle diameter. The single drop experiments clearly show an increase of the breakage time with increasing particle diameter as proposed only by Coulaloglou and Tavlarides (1977). On the other hand the values for used PBE breakage time terms in the literature are at least one magnitude higher than those found here experimentally. The experimental single drop breakage time results are in very good agreement with earlier experimental studies in the literature. Therefore, we propose to evaluate carefully the use of model constants which determine the breakage time in the PBE.

Different value combinations for those model constants can be used to describe the same set of experiments with one model. That shows that fitting of PBE parameters is a major challenge. Additionally, many physical influence parameters on drop sizes are still not implemented in the models or described properly. This all leads to a broad variety of parameters that are briefly summarized in the Appendix A.

To include two different breakage mechanisms and additional physical properties in one model, a new breakage time approach was derived. This model takes the elongation of drops and the turbulent pressure fluctuations on the drop surfaces into account. By using a critical diameter for the elongation-based breakage, the viscosity of the dispersed phase as the interfacial tension between the two phases was introduced in the modeling of the breakage time. This model was combined with different breakage probabilities. The combination of the new breakage time with the breakage probability of Chen et al. (1998) was able to reflect the experimental results from the single drop experiments very satisfactory. These new breakage rates have been tested in simulations of liquid-liquid applications which will bepresented in further studies.

ACKNOWLEDGEMENTS

The authors gratefully acknowledge the efficient support by the DAAD students Ms. Sarah Turner and Ms. Jennifer Komaiko, as well as the DAAD for the financial support via the RISE program and Ms. Gottschling for great cooperation over the last few years. We additionally thank Ms. Melanie Zillmer for the full automation of the image analysis.

This work was financially supported by the “Max-Buchner-Forschungsstiftung.”

LATIN SYMBOLS

c	concentration [g/L]
c	proportionality or numerical constant [various]
Ca	Capillary number [-]
d_{32}	Sauter mean diameter [m]
d_P, d_i	particle, mother drop diameter [m]
d'_P, d''_P	daughter drop diameter of the first and the second daughter drop [m]
D	stirrer diameter [m]
$D_\square$	flow cell characteristic length [m]
g	breakage rate [1/s]
H	liquid level of the stirred vessel [m]
n_0	relative number distribution [-]

n	stirrer speed [rpm]
N	number [-]
Oh	Ohnesorge number [-]
P	breakage probability [-]
Re	Reynolds number [-]
T	vessel diameter [m]
t	time [s]
t_b	breakage time [s]
$t_{b,av}$	arithmetic average breakage time [s]
$t_{b,\beta}$	peak value of the β-distribution of the breakage time [s]
u'	turbulent fluctuation velocity [m/s]
V	variance [various]
V_r	investigated volume of the breakage cell [m^3]
$\dot{V}$	volume flow rate [L/s]
w	flow velocity [m/s]
w_{tip}	stirrer tip velocity [m/s]
We	Weber number [-]

GREEK SYMBOLS

β	daughter drop size distribution [-]
γ	interfacial tension [N/m]
ε	energy dissipation rate [m^2/s^3]
$\dot{\varepsilon}$	elongation rate [1/s]
η	dynamic viscosity [Pa·s]
λ	viscosity ratio [-]
ν	number of daughter drops [-]
ρ	density [kg/m^3]
σ	standard deviation [various]
φ	dispersed phase fraction [-]

SUBSCRIPTS

av	average
b	breakage
c	continuous
crit	critical
d	dispersed
dr	drop
e	elongation
exp	experiment
max	maximum
mod	model
P	particle
res	residence
str	stirrer
turb	turbulent

ABBREVIATIONS

2D	two dimensional
3D	three dimensional
C&T (1977)	Coulaloglou and Tavlarides (1977)
fps	frames per second
PBE	population balance equation

APPENDIX A

Table 8 – parameter listing

Literature reference	model displayed in equation	$c_{1,b}$	$c_{2,b}$	$c_{3,b}$
model from Coulaloglou and Tavlarides (1977)				
Coulaloglou and Tavlarides 1977	(6)	$3.36 \cdot 10^{-1}$	$1.06 \cdot 10^{-1}$	-
Gäbler et al. 2006	(6)	$6.14 \cdot 10^{-4}$	$5.70 \cdot 10^{-2}$	-
Azizi and Al Taweel 2011	(6)	$8.6 \cdot 10^{-1}$	$4.1 \cdot 10^{0}$	-
this study	(6)	$9.1 \cdot 10^{-1}$	$3.9 \cdot 10^{-1}$	-
model from Chen et al. (1998)				

Chen et al. 1998	(9)	$6.04 \cdot 10^{-1}$	$1.14 \cdot 10^{-3}$	$7.85 \cdot 10^{-3}$
Ruiz and Padilla 2004	(9)	$4.40 \cdot 10^{-1}$	$5.00 \cdot 10^{-3}$	$5.00 \cdot 10^{-3}$
this study	(9)	not determined	$3.9 \cdot 10^{-1}$	$7.85 \cdot 10^{-3}$
model from Alopaeus et al. (2002)				
Alopaeus et al. 2002	(11)	$3.68 \cdot 10^{0}$	$7.75 \cdot 10^{-2}$	$2.00 \cdot 10^{-1}$
Gäbler et al. 2006	(11)	$3.63 \cdot 10^{-3}$	$2.49 \cdot 10^{-4}$	$7.24 \cdot 10^{-2}$
Singh et al. 2009	(11)	$7.70 \cdot 10^{0}$	$1.50 \cdot 10^{-2}$	$1.00 \cdot 10^{-2}$
this study	(11)	$1.6 \cdot 10^{2}$	$1.6 \cdot 10^{-1}$	$2.00 \cdot 10^{-1}$

APPENDIX B

Table 9 – experimentally achieved breakage probabilities of single toluene and single petroleum drops at a superficial velocity of 1.5 m/s

mother drop diameter d_P [mm]	toluene		petroleum	
	P [-]	σ [%]	P [-]	σ [%]
0.54	-	-	0.19	11.1
0.66	0.45	6.2-	-	-
0.70	-	-	0.50	6.9
1.00	0.60	5.0	0.55	6.8
1.30	-	-	0.58	5.7
1.90	-	-	-	-
2.00	0.75	2.7	0.78	6.3
3.00	0.81	2.9	-	-
3.10	-	-	0.82	3.2

APPENDIX C

Table 10 – experimentally achieved breakage times of single toluene and single petroleum drops at a superficial velocity of 1.5 m/s

mother drop diameter d_P [mm]	arithmetic average values				peak values of the β-distribution			
	toluene		petroleum		toluene		petroleum	
	$t_{b,av}$ [ms]	σ [ms]	$t_{b,av}$ [ms]	σ [ms]	$t_{b,\beta}$ [ms]	σ [%]	$t_{b,\beta}$ [ms]	σ [%]
0.54	-	-	34.0	3.5	-	-	2.7	10.4
0.66	19.7	2.6	-	-	2.5	13.2	-	-
0.70	-	-	23.5	4.3	-	-	3.4	18.3
1.00	12.4	5.4	16.0	1.0	3.4	43.2	4.7	6.4
1.30	-	-	14.9	0.7	-	-	8.3	4.9
1.90	-	-	13.9	0.6	-	-	9.9	4.2
2.00	14.3	0.9	-	-	8.9	6.2	-	-
3.00	16.1	0.41	-	-	11.6	2.5	-	-
3.10	-	-	16.6	1.0	-	-	13.3	6.1

LITERATURE

Abramowitz, M., Stegun, I.A. and Danos, M., 1984. Pocketbook of mathematical functions. Handbook of mathematical functions. Harri Deutsch, Frankfurt (Main), 468 pp.

Alopaeus, V., Koskinen, J., Keskinen, K.I. and Majander, J., 2002. Simulation of the population balances for liquid-liquid systems in a nonideal stirred tank. Part 2 - Parameter fit-

ting and the use of the multiblock model for dense dispersions. Chemical Engineering Science, 57(10): 1815-1825.

Andersson, R., Andersson, B., Chopard, F. and Noren, T., 2004. Development of a multi-scale simulation method for design of novel multiphase reactors. Chemical Engineering Science, 59(22-23): 4911-4917.

Andersson, R. and Andersson, B., 2006. On the breakup of fluid particles in turbulent flows. AIChE Journal, 52(6): 2020-2030.

Azizi, F. and Al Taweel, A.M., 2011. Turbulently flowing liquid-liquid dispersions. Part I: Drop breakage and coalescence. Chemical Engineering Journal, 166(2): 715-725.

Bahmanyar, H. and Slater, M.J., 1991. Studies of drop break-up in liquid-liquid systems in a rotating disc contactor. Part I: Conditions of no mass transfer. Chemical Engineering and Technology, 14(2): 79-89.

Batchelor, G.K., 1952. Diffusion in a field of homogeneous turbulence: II. The relative motion of particles. Mathematical Proceedings of the Cambridge Philosophical Society, 48: 345-362.

Calabrese, R.V., Chang, T.P.K. and Dang, P.T., 1986. Drop Breakup in Turbulent Stirred-Tank Contactors .1. Effect of Dispersed-Phase Viscosity. AIChE Journal, 32(4): 657-666.

Chen, Z., Prüss, J. and Warnecke, H.J., 1998. A population balance model for disperse systems: Drop size distribution in emulsion. Chemical Engineering Science, 53(5): 1059-1066.

Coulaloglou, C.A. and Tavlarides, L.L., 1977. Description of Interaction Processes in Agitated Liquid-Liquid Dispersions. Chemical Engineering Science, 32(11): 1289-1297.

Eastwood, C.D., Armi, L. and Lasheras, J.C., 2004. The breakup of immiscible fluids in turbulent flows. Journal of Fluid Mechanics, 502: 309-333.

Gäbler, A., Wegener, M., Paschedag, A.R. and Kraume, M., 2006. The effect of pH on experimental and simulation results of transient drop size distributions in stirred liquid-liquid dispersions. Chemical Engineering Science, 61(9): 3018-3024.

Galinat, S., Masbernat, O., Guiraud, P., Dalmazzone, C. and Noik, C., 2005. Drop break-up in turbulent pipe flow downstream of a restriction. Chemical Engineering Science, 60(23): 6511-6528.

Gourdon, C. and Casamatta, G., 1991. Influence of mass-transfer direction on the operation of a pulsed sieve-plate pilot column. Chemical Engineering Science, 46(11): 2799-2808.

Haggag, A.A., 1981. A Variant of the Generalized Reduced Gradient Algorithm for Non-Linear Programming and Its Applications. European Journal of Operational Research, 7(2): 161-168.

Hesketh, R.P., Etchells, A.W. and Russell, T.W.F., 1991. Experimental-Observations of Bubble Breakage in Turbulent-Flow. Industrial and Engineering Chemistry Research, 30(5): 835-841.

Jon, D.I., Rosano, H.L. and Cummins, H.Z., 1986. Toluene Water/1-Propanol Interfacial-Tension Measurements by Means of Pendant Drop, Spinning Drop, and Laser Light-Scattering Methods. Journal of Colloid and Interface Science, 114(2): 330-341.

Konno, M., Aoki, M. and Saito, S., 1983. Scale Effect on Breakup Process in Liquid Liquid Agitated Tanks. Journal of Chemical Engineering of Japan, 16(4): 312-319.

Kumar, S., Ganvir, V., Satyanand, C., Kumar, R. and Gandhi, K.S., 1998. Alternative mechanisms of drop breakup in stirred vessels. Chemical Engineering Science, 53(18): 3269-3280.

Lasheras, J.C., Eastwood, C., Martínez-Bazán, C. and Montanés, J.L., 2002. A review of statistical models for the break-up of an immiscible fluid immersed into a fully developed turbulent flow. International Journal of Multiphase Flow, 28(2): 247-278.

Levich, V.G., 1962. Physicochemical Hydrodynamics. The Physical and Chemical Engineering Sciences. Prentice-Hall, Inc., Englewood Cliffs, N. J., 700 pp.

Liao, Y. and Lucas, D., 2009. A literature review of theoretical models for drop and bubble breakup in turbulent dispersions. Chemical Engineering Science, 64(15): 3389-3406.

Liao, Y. and Lucas, D., 2010. A literature review on mechanisms and models for the coalescence process of fluid particles. Chemical Engineering Science, 65(10): 2851-2864.

Maaß, S., Gäbler, A., Zaccone, A., Paschedag, A.R. and Kraume, M., 2007. Experimental investigations and modelling of breakage phenomena in stirred liquid/liquid systems. Chemical Engineering Research and Design, 85(A5): 703-709.

Maaß, S., Wollny, S., Sperling, R. and Kraume, M., 2009. Numerical and experimental analysis of particle strain and breakage in turbulent dispersions. Chemical Engineering Research and Design, 87(4): 565–572.

Maaß, S., Metz, F., Rehm, T. and Kraume, M., 2010. Prediction of drop sizes for liquid-liquid systems in stirred slim reactors - Part I: Single stage impellers. Chemical Engineering Journal, 162(2): 792-801.

Maaß, S., Wollny, S., Voigt, A. and Kraume, M., 2011a. Experimental comparison of measurement techniques for drop size distributions in liquid/liquid dispersions. Experiments in Fluids, 50(2): 259-269.

Maaß, S., Rehm, T. and Kraume, M., 2011b. Prediction of drop sizes for liquid-liquid systems in stirred slim reactors - Part II: Multiple stage impellers. Chemical Engineering Journal, 168(2): 827–838.

Mietus, W.G.P., Matar, O.K., Lawrence, C.J. and Briscoe, B.J., 2002. Droplet deformation in confined shear and extensional flow. Chemical Engineering Science, 57(7): 1217-1230.

Narsimhan, G., Gupta, J.P. and Ramkrishna, D., 1979. Model for Transitional Breakage Probability of Droplets in Agitated Lean Liquid-Liquid Dispersions. Chemical Engineering Science, 34(2): 257-265.

Raikar, N.B., Bhatia, S.R., Malone, M.F. and Henson, M.A., 2009. Experimental studies and population balance equation models for breakage prediction of emulsion drop size distributions. Chemical Engineering Science, 64(10): 2433-2447.

Ramkrishna, D., 2000. Population balances, theory and applications to particulate systems in engineering. Academic Press, San Diego, CA, 355 pp.

Ribeiro, M.M., Regueiras, P.F., Guimaraes, M.M.L., Madureira, C.M.N. and Pinto, J., 2011. Optimization of breakage and coalescence model parameters in a steady-state batch agitated dispersion. Industrial & Engineering Chemistry Research, 50(4): 2182-2191.

Risso, F. and Fabre, J., 1998. Oscillations and breakup of a bubble immersed in a turbulent field. Journal of Fluid Mechanics, 372: 323-355.

Ross, S.M., 1983. Stochastic processes. Wiley series in probability and mathematical statistics / Probability and mathematical statistics. Wiley, New York, 309 pp.

Ruiz, M.C. and Padilla, R., 2004. Analysis of breakage functions for liquid-liquid dispersions. Hydrometallurgy, 72(3-4): 245-258.

Schmidt, S.A., Simon, M., Attarakih, M.M., Lagar, L. and Bart, H.M., 2006. Droplet population balance modelling - hydrodynamics and mass transfer. Chemical Engineering Science, 61(1): 246-256.

Shinnar, R., 1961. On the Behaviour of Liquid Dispersions in Mixing Vessels. Journal of Fluid Mechanics, 10(2): 259-275.

Singh, K.K., Mahajani, S.M., Shenoy, K.T. and Ghosh, S.K., 2009. Population balance modeling of liquid-liquid dispersions in homogeneous continuous-flow stirred tank. Industrial and Engineering Chemistry Research, 48(17): 8121-8133.

Stoots, C.M. and Calabrese, R.V., 1995. Mean velocity-field relative to a Rushton turbine blade. AIChE Journal, 41(1): 1-11.

Stork, M., 2005. Model-based optimization of the operation procedure of emulsification. dissertation Thesis, Technical University Delft, Delft, 181 pp.

Taylor, G.I., 1934. The formation of emulsions in definable fields of flow. Proceedings of the Royal Society of London. Series A, Containing Papers of a Mathematical and Physical Character, 146(858): 501-523.

Tsouris, C. and Tavlarides, L.L., 1994. Breakage and coalescence models for drops in turbulent dispersions. AIChE Journal, 40(3): 395-406.

Vankova, N., Tcholakova, S., Denkov, N.D., Vulchev, V.D. and Danner, T., 2007. Emulsification in turbulent flow 2. Breakage rate constants. Journal of Colloid and Interface Science, 313(2): 612-629.

Villermaux, E., 2007. Fragmentation. Annual Review of Fluid Mechanics, 39: 419-446.

Walstra, P., 1993. Principles of Emulsion Formation. Chemical Engineering Science, 48(2): 333-349.

Wichterle, K., 1995. Drop Breakup by Impellers. Chemical Engineering Science, 50(22): 3581-3586.